Final Report for
Grant DE-FG02-91ER40690
for the period 12/1/2010 to 4/30/2014

Task A: (CMS)
Task B: (Theoretical Studies)
Task D: (ATLAS)
Task E: (CDF, CMS, FERMI)
Task R: (BaBar, e^+e^-)
Task X: (BOSS, DES)

The Ohio State University
Department of Physics
The Ohio State University
191 West Woodruff Ave
Columbus, Ohio 43210

July, 2014

This is the final report for The Ohio State University high energy physics grant DE-FG02-91ER40690. The activities of the various Tasks are briefly summarized over the previous grant period. The support from the Department of Energy is greatly appreciated.

DE-FG02-91-ER40690 Final Report

Office of High Energy Physics
Technical Contact: Abid Patwa
The Ohio State University
Dept. of Physics
191 W. Woodruff Ave., Columbus, OH 43210-1117

Task A

Research in elementary particle physics with the CMS Experiment

---

Principal Investigators:

L.S. Durkin* and C.S. Hill

1 Introduction to Task A

The Ohio State CMS group conducts research at the Energy Frontier with the Compact Muon Solenoid (CMS) experiment at CERN's Large Hadron Collider (LHC). During the majority of the time spanned by this final report (2010–2014) the activities on the CMS experiment were divided between "Task A" and "Task E". In this period, the personnel of the Task A consisted of two faculty members (Stan Durkin, Chris Hill), three postdocs, one engineer/physicist supported by the US CMS M&O program and five graduate students (one of whom graduated in 2011). A significant portion of this group was resident at CERN. The final report on contributions to CMS by two other OSU faculty members (Richard Hughes, Brian Winer) are contained in the Task E write-up.

2 Final Report on Task A M&O/Upgrade Activities, 2010–2014

In this period, Ohio State were heavily involved in all aspects of the CSC muon subsystem. Under Durkin's leadership, the CSC electronics system was delivered on time and within budget. The installed system was extensively tested during commissioning and shown to perform according to design specifications. OSU engineer Bylsma won a CMS lifetime achievement award in recognition of this effort. Task A personnel from both Durkin and Hill's groups played crucial roles in the operation of the CSC electronics system and online software at CERN. In addition to detector maintenance responsibilities, this effort has made several contributions to event reconstruction code such as fitting of pulse heights, timing of CSC hits, and forming muon track segments. The group also played a leading role in the upgrade of the CSC ME1/1 electronics. Task A also contributed to the CMS upgrade more generally. Hill served a term as deputy physics coordinator from 2012-2014; one of his responsibilities during this period was to lead the effort carrying out the physics studies in support of the Phase 1 and Phase 2 CMS upgrade programs.

2.1 Operations

As well as taking its share of CSC DQM shifts, OSU was responsible for a very large part of the CSC electronics. Diagnosing and fixing electronics problems on the detector was a demanding task. Most members of the group were listed as CSC system experts who were called to fix problems found with electronics during LHC running. There were approximately three of these calls per week. As an example, during a high intensity pileup test run before the Christmas shutdown in 2011, the CSC data acquisition system encountered a large number of L1A out-of-sync errors, stopping global running. The source of the problem was traced to rare loss-of-link conditions on the dual rocket-io 3.2 Gbps links between each DDU and the DCC in each crate. Consequently, during the 2011 shutdown, an extensive upgrade of the DDU/DCC firmware was performed that fixed the problem. Between 2011–2012, Rodenburg took 16 weeks of shifts as the CSC Data-On-Call (DOC) expert. A CSC DOC takes total responsibility for 24 hour running of the CSC system.

2.2 ME1/1 Electronics Upgrade

In 2009 Durkin proposed a Phase I electronics upgrade for the inner ring of the first CSC station (ME1/1). Since ME1/1 has the highest particle rates in the muon system, the CSC radial strips are divided into inner and outer sub-chambers. To save electronics costs the inner sub-chamber strips were ganged modulo 3 to reduce the number of electronics boards. This last decision has proven problematic for the global muon trigger causing large trigger rates due to the resulting ghost tracks. In addition at HL-LHC input rates, overuse of the front-end electronic's switch capacitor arrays (96 capacitors per channel) will result in significant dead-time in the cathode data readout. The upgraded ME1/1 electronics system solved both of these long term problems.

The scale of the ME1/1 electronics upgrade was large, requiring 840 new electronics boards of 5 different types. The universities collaborating in the upgrade were: OSU, UCSB, TAMU, UCLA, Rice, Wisconsin, and UCD. The key component of the new electronics, the Digital Cathode Front End Board (DCFEB), was designed and built by Ohio State. The DCFEB uses newly available technology to create a nearly dead-timeless front-end board. Flash ADC's are used for each channel on the DCFEB and FPGA digital memories replace the old front-end-boar SCA's. In addition the trigger primitives and data are now transmitted optically to the peripheral crates, eliminating transfer errors in the old CFEB channel links/copper cable interface.

Over the past three years, this Ohio State group spent a large portion of their effort on the designing, testing, and production of the DCFEB boards for the ME1/1 Level I upgrade. An R&D prototype was completed mid-2011 and tested in 2012. It proved so successful that a second R&D prototype was considered unnecessary. Ten preproduction prototypes of the DCFEB boards, with fully tested firmware and software, were delivered in June of 2012. All parts on the board were radiation tested by the OSU group at the Crocker Lab at UC Davis. Extensive work was done developing firmware and communications software ($\sim$ 20K lines of C code) during this period. After extensive tests at OSU and CERN point 5, a production readiness review on December 4, 2012 recommended production of the boards. The production and testing of the 554 boards began in late May of 2013, and the last boards were shipped to CERN in December of 2013. The CFEB electronics boards recovered during the installation of the ME1/1 upgrade electronics will populate the new ME4/2 chambers that have been constructed at CERN.

2.3 Upgrade Physics Coordination

As noted above, Hill was charged with coordinating physics studies that support planned and proposed upgrades to the CMS experiment, and providing input to national/international strategy groups that will chart the long-term future of particle physics. This was not a small task, given that in many cases the details of the proposed modifications to the detector were not settled (much less was there any reconstruction code written to take advantage of the upgrades). It was, however, vital to overcome these obstacles since physics input was crucial to make informed decisions about how the experiment (and HEP in general) should proceed in the post Higgs discovery era. The period 2012–2013 was a busy time for this type of activity, as there were a number of important documents solicited by various agencies to which Hill made significant contributions. These included the CMS submission to the European Strategy for Particle Physics [1], the CMS "whitepaper" submitted to

the Snowmass community planning process [2], three technical design reports (TDRs) for proposed Phase 1 upgrades: the first detailing the design and expected performance of the upgraded pixel detector [3] that will have less material despite adding a fourth layer, the second did the same for upgraded hadron calorimeter [4] that will have new photodetectors and longitudinal segmentation, and the third demonstrating the need for and expected performance of an updated, more flexible, L1 trigger system [5].

3 Final Report on Task A Data Analysis Activities, 2010–2014

In the summer of 2012, the CMS collaboration announced the observation of a new boson with a mass near 125 GeV/c^2. Follow up studies support the interpretation that that this new particle is a Higgs boson. With the apparent discovery of the Higgs, searches for new physics beyond the Standard Model have taken on a new urgency. The question as to whether there is a "natural" mechanism stabilizing the Higgs mass at this value (since in QFT such scalars are inherently unstable due to quadratic quantum corrections) or we simply live in a fine-tuned universe has moved from a theoretical consideration to a very real experimental problem. Moreover, since all searches to date for such natural solutions (e.g. supersymmetry, extra dimensions) have returned null results, searches for experimentally challenging scenarios that could have eluded these searches have become of paramount importance. The OSU CMS group performed a number of such BSM searches leading to the publications listed in the Appendix.

3.1 Searches for Stopped Heavy Particles

Many extensions to the SM of particle physics predict the existence of new heavy quasi-stable charged particles with lifetimes much longer than typical LHC experimental timescales. During 2007-9, Hill pioneered a non-traditional search for any such long-lived particles that might have become stopped by the CMS detector. In order to record such decays, Hill devised, implemented, and commissioned a novel calorimeter trigger that fires on the energy deposited during the decay of these stopped particles during the gaps between the proton bunches in the LHC (hence avoiding pp collision backgrounds). In 2011, Ohio State led the analysis of the data recorded by Hill's trigger during the 2010 run of the LHC, the results of which were published in [6]. In 2012, Ohio State analyzed the corresponding data from the 2011 run of the LHC. These results considerably extended constraints obtained from previous stopped particle searches and were published in [7].

3.2 Search for Charge Asymmetric W' Production

The top quark is interesting not only because it the heaviest fundamental particle but also because (somewhat as a result of this) top quarks often play a significant role in many extensions to the SM. Moreover, the observation by the CDF and D0 experiments of an anomalously large forward-backward asymmetry further motivated performing searches for new physics in the top sector. In particular, N. Craig et al, in Phys. Rev. D84:035012 (2011) suggested that the observed anomaly could be due to a maximally flavor violating W' model which would couple tops to down quarks.

In this model, it is therefore possible to produce top quark pairs in association with a jet through t-channel exchange of the W' or via s-channel exchange of a d-quark. Ohio State together with collaborators from Rutgers, performed such an analysis on the 2011 LHC data. We neither observed a significant excess above SM background expectations in the counting experiment, nor did we see evidence of the expected charge asymmetry in the reconstruction analysis. W' masses below 840 GeV were excluded, ruling out this particular explanation for the Tevatron forward-backward asymmetry. The analysis was published in [8].

3.3 Searches for Fractionally Charged Particles

In Phys. Lett. B717:351?370 (2012), P. Meade et al suggested that BSM physics scenarios could manifest themselves as particles whose trajectories could be difficult to reconstruct and are therefore overlooked in current collider experiments. At Ohio State, we performed a search for one such class of these tracks, namely those produced by fractionally charged particles. Since the ionization energy recorded by the CMS silicon tracker ("dE/dx") is proportional to the square of the charged particle traversing the active area, fractionally charged particles would produce tracks with hits with significantly lower dE/dx than ordinary charged particles. Zero events with such tracks were observed in the search sample, consistent with the background estimate of 0.012 ± 0.007 events. We set upper limits on the cross section of pair-produced, spin-1/2 particles that are neutral under $SU(3)_C$ and $SU(2)_L$. These limits excluded with 95% confidence such particles with electric charge $\pm 2e/3$ with masses below 310 GeV, and those with $\pm e/3$ with masses below 140 GeV. This analysis was published in [9]. In 2013, a variation on this search was performed on the 18.8 fb^{-1} 8 TeV data sample collected in 2012. In this updated analysis, the search for fractionally charged particles is presented in conjunction with searches for other anomalous dE/dx signals arising from particles with electric charge equal to or greater than that of the electron. With the combination of the 7 TeV and 8 TeV data samples, the excluded masses are extended to 480 (200) GeV for particles with charge $\pm 2e/3$ ($\pm e/3$) respectively. This paper was published in [10].

3.4 Search for RPV/Stealth SUSY

Two possible manifestations of natural supersymmetry that were not sufficiently tested by direct searches from the LHC experiments were R-parity violating (RPV) and "stealth" SUSY scenarios. In 2013, Ohio State with collaborators from Rutgers university, performed an analysis that was sensitive to both of these. In particular, this search targeted an RPV gluino model and a stealth SUSY model with a sbottom decaying to a stealth singlino, singlet, and gravitino. The analysis employed a technique in which all possible 3-jet mass ensembles are formed from the six highest-p_T jets. There are thus 20 possible triplets, two of which could contain a signal resonance. To find the correctly reconstructed triplets, the triplet sum p_T is plotted vs. triplet mass and a diagonal cut was made. Below this diagonal cut, correctly reconstructed triplets were enriched. A fit to the distribution of the triplet masses surviving this cut was then performed to extract the resonant signal (if present) from the broad combinatoric background. The result of this fit on 19.5 fb^{-1} showed no significant presence of a signal and excluded RPV gluinos with masses up to about 835 GeV at 95% C.L. These results were the most stringent such constraints to date and were published in [11].

Appendix: Task A Publications, 2010–2014

[1] CMS at the High-Energy Frontier. Contribution to the Update of the European Strategy for Particle Physics. Technical Report CMS-NOTE-2012-006, CERN, 2012.

[2] Projected Performance of an Upgraded CMS Detector at the LHC and HL-LHC: Contribution to the Snowmass Process. Technical Report CMS-NOTE-13-002, 2013.

[3] CMS Technical Design Report for the Pixel Detector Upgrade. Technical Report CERN-LHCC-2012-016, 2012.

[4] CMS Technical Design Report for the Phase 1 Upgrade of the Hadron Calorimeter. Technical Report CERN-LHCC-2012-015, 2012.

[5] CMS Technical Design Report for the Level-1 Trigger Upgrade. Technical Report CMS-TDR-012, 2013.

[6] Vardan Khachatryan et al. Search for Stopped Gluinos in pp collisions at $\sqrt{s} = 7$ TeV. *Phys.Rev.Lett.*, 106:011801, 2011.

[7] Serguei Chatrchyan et al. Search for stopped long-lived particles produced in pp collisions at $\sqrt{s} = 7$ TeV. *JHEP*, 1208:026, 2012.

[8] Serguei Chatrchyan et al. Search for charge-asymmetric production of W' bosons in top pair + jet events from pp collisions at $\sqrt{s} = 7$ TeV. *Phys.Lett.*, B717:351–370, 2012.

[9] S. Chatrchyan et al. Search for fractionally charged particles in pp collisions at $\sqrt{s} = 7$ TeV. *Phys. Rev. D*, 87:092008, May 2013.

[10] Serguei Chatrchyan et al. Searches for long-lived charged particles in pp collisions at $\sqrt{s}$=7 and 8 TeV. *JHEP*, 1307:122, 2013.

[11] Serguei Chatrchyan et al. Searches for light- and heavy-flavour three-jet resonances in pp collisions at $\sqrt{s} = 8$ TeV. *Phys.Lett.*, B730:193–214, 2014.

FINAL REPORT

on Department of Energy grant

DE-FG02-91ER40690 (Task B)

for the period

Dec. 1 2010 – April 30 2014

Eric Braaten

Samir Mathur

Stuart Raby

Junko Shigemitsu

High Energy Physics Group
The Ohio State University

1 High Energy Theory Group

The High Energy Theory Group at the Ohio State University has a broad research program that covers many of the most important areas of high energy theory. The group is supported by the Division of High Energy Physics of the Department of Energy. This Final Report covers the activities of the group during the most recent funding period from December 1 2010 to April 2014.

Faculty

The High Energy Theory Group includes four faculty: **Eric Braaten**, **Samir Mathur**, **Stuart Raby**, and **Junko Shigemitsu**. Their research reports, including lists of publications since 2011, are presented below.

During the academic year 2011/12, the Physics Department completed a successful faculty search in Theoretical Particle Physics. **Linda Carpenter** from the University of California, Irvine, joined the department in Autumn 2012 as assistant professor. Carpenter, whose expertise is in LHC phenomenology and physics beyond the Standard Model, significantly broadens and strengthens the particle physics program at Ohio State. She is currently applying for research support from several funding agencies, including the Department of Energy.

Postdocs and Students

The High Energy Theory Group also includes postdoctoral research associates and graduate students. The postdocs that have been supported by the group since 2011 are as follows:

- **Heechang Na**, who worked with Shigemitsu, moved on to a postdoctoral position at Argonne in 2011,
- **Konstantin Bobkov**, who worked with Raby,
- **Pierre Artoisenet**, who worked with Braaten, moved on to a postdoctoral position at NIKHEF in 2011,
- **Chris Bouchard**, who is currently working with Shigemitsu,
- **David Turton**, who is currently working with Mathur.

The graduate students that have been supported by the group since 2011 are as follows:

- **Archana Anandakrishnan**, whose advisor is Raby, will receive her Ph.D. in 2015.
- **Zachary Carson**, whose advisor is Mathur. will receive his Ph.D. in 2016.
- **Brandon Bryant**, whose advisor is Raby, is just begining his Ph.D. research.

2 Eric Braaten

My research involves the use of quantum field theory to solve problems in diverse areas of physics. Two recurring themes in my work are the use of *effective field theory* to separate the effects of different scales and the use of *resummation methods* to extend the applicability of perturbation theory.

In the summer of 2013, I organized the writing of a Snowmass White Paper on quarkonium physics entitled *Quarkonium at the Frontiers of High Energy Physics*. This 43-page document with 6 authors describes the opportunities for dramatic progress in two specific areas: the spectrosocopy of quarkonium above the open-heavy-flavor thresholds, where progress is being driven by experiments at the Intensity Frontier, and the production of quarkonium at large transverse momentum, where progress is being driven by experiments at the Energy Frontier. These two areas of quarkonium physics have been the primary foci of my research in high energy physics in recent years. I have also recently branched out into dark matter physics, where I have been exploring the possibility that dark matter particles might have strong interactions at low energy.

Production of Heavy Quarkonium

The production of heavy quarkonium in high energy collisions is a problem that should be amenable to analysis using perturbative QCD. In 1994, Bodwin, Lepage, and I developed a systematic method for calculating annihilation decay rates and inclusive production rates for heavy quarkonium called *NRQCD factorization*. The important momentum scales in quarkonium include the heavy quark mass m_Q and the typical relative momentum $m_Q v$. NRQCD factorization uses an effective field theory called NonRelativistic QCD to factor rates into long-distance factors that involve only momenta of order $m_Q v$ or smaller and short-distance factors that involve only momenta of order m_Q and larger. The long-distance factors are nonperturbative but universal, while the short-distance factors can be calculated as perturbation series in $\alpha_s(m_Q)$.

Over the last decade, several groups carried out heroic calculations of all the short-distance factors in the cross sections for quarkonium production to next-to-leading order (NLO) in α_s. These corrections, which in many cases are large, have removed most of the discrepancies between NRQCD factorization and experiment, but there are still some dramatic discrepancies in polarization observables. NRQCD factorization predicts that $J^{PC} = 1^{--}$ quarkonium states, such as J/ψ and Υ, should be mostly transversely polarized at sufficiently large transverse momentum p_T, because their production is dominated by gluon fragmentation into a color-octet $Q\bar{Q}$ pair. Measurements of the polarization at the Tevatron and the LHC seem to be in dramatic disagreement with this prediction. Russ and I recently wrote a review of the polarization of J/ψ and Υ in hadronic production processes.

A dramatic new theoretical development in quarkonium production was made in 2011 by Kang, Qiu, and Sterman. They proved that factorization holds at large p_T through next-to-leading order in m_Q^2/p_T^2. This motivates a reorganization of the quarkonium cross section from a strict expansion in α_s, with coefficients that are functions of m_Q/p_T, to an expansion in m_Q^2/p_T^2, with coefficients that are expansions in powers of α_s. I am optimistic that this reorganization will decrease the size of the NLO corrections and also solve the remaining phenomenological problems, such as the polarization at large p_T. The leading terms in the

expansion in m_c^2/p_T^2 are given by the fragmentation functions for partons to hadronize into quarkonium. I calculated most of the relevant fragmentation functions to leading order in α_s in the early 1990's. This new reorganization of quarkonium cross sections makes it worthwhile to extend those calculations to NLO. I have therefore launched a program with Pierre Artoisenet to calculate all the fragmentation functions for quarkonium to NLO. Although we have made significant progress, this work has not yet led to any published papers. Measurements of the cross sections at large p_T at the LHC should provide rigorous tests of this new framework for quarkonium production.

Quarkonium above the Open-Flavor Threshold

In the last decade, there has been dramatic progress in the spectroscopy of mesons containing a heavy quark and antiquark from experiments at the charm and bottom factories. All the states in the charmonium and bottomonium multiplets below the open-heavy-flavor thresholds have now been discovered. However dozens of new states above the open-heavy-flavor thresholds have also been discovered and many of them have properties that are incompatible with ordinary quarkonium ($Q\bar{Q}$). These new states are referred to as XYZ mesons. Some of them are definitely tetraquarks ($Q\bar{Q}q\bar{q}$), because they are electrically charged. Others may be quarkonium hybrids ($Q\bar{Q}g$), which have a gluonic excitation. Lattice QCD may eventually be able to elucidate the nature of many of these quarkonium-like states, but it is only beginning to be brought to bear on this problem. Moreover there are some aspects of this problem that will never be tractible using lattice methods but could be attacked using effective field theory methods.

The first XYZ meson to be discovered was the $X(3872)$, discovered by the Belle collaboration in 2003. Measurements of the mass of the $X(3872)$ indicate that it is within 1 MeV of the $D^{*0}\bar{D}^0$ threshold. Its J^{PC} quantum numbers have recently been determined definitively by the LHCb collaboration to be 1^{++}, which allows an S-wave coupling to $D^{*0}\bar{D}^0$. The universality of S-wave threshold resonances then implies that the $X(3872)$ must be a loosely-bound *charm meson molecule*, whose constituents are a superposition of $D^{*0}\bar{D}^0$ and $D^0\bar{D}^{*0}$ with a large mean separation between the charm mesons. I have been trying to make the case that the $X(3872)$ is a charm meson molecule since shortly after its discovery. Artoisenet and I pointed out the flaw in a theory paper that argued that the production rate of the $X(3872)$ at the Tevatron and the LHC is orders of magnitude too large for it to be a charm-meson molecule. Kang and I pointed out a flaw in a Babar analysis that favored the quantum numbers 0^{-+} over 1^{++}. I will continue to make the case for the identification of the $X(3872)$ as a charm meson molecule until it is universally accepted.

As more and more XYZ mesons were discovered over the last decade, I became increasingly mystified at how they could be understood within QCD. Among the most mystifying were the $Y(4260)$ discovered by the Babar collaboration in 2005, the $Z_b^+(10610)$ and $Z_b^+(10610)$ discovered by the Babar collaboration in 2010, and the $Z_c^+(3900)$ discovered by the BESIII collaboration in 2013. These Z_b^+ and Z_c^+ mesons have electric charge, so they must be quarkonium tetraquark mesons with constituents $b\bar{b}u\bar{d}$ and $c\bar{c}u\bar{d}$, respectively.

In 2013, I finally had an inspiration that I believe provides the solution to the nature of the XYZ states. The key is the *Born-Oppenheimer approximation*, which was pioneered in QCD by Juge, Kuti, and Morningstar around 2000, but was not developed much further. Born-Oppenheimer (B-O) potentials in QCD can be defined as energies of gluon and light-quark fields in the presence of static Q and $\bar{Q}$ sources. In the Born-Oppenheimer approximation, the

Q and $\bar{Q}$ move in accord with the Schroedinger equation in the B-O potential, while the gluon and light-quark fields respond instantaneously to the motion of the Q and $\bar{Q}$. Conventional quarkonia correspond to solutions of the Schroedinger equation in the lowest B-O potential. Quarkonium hybrids can be identified with solutions of the Schroedinger equation in excited B-O potentials. My inspiration was the realization that the quarkonium tetraquarks can be identified with solutions of the Schroedinger equation for the Q and $\bar{Q}$ in B-O potentials defined by energies of gluon and light-quark fields with isospin 1. The discoveries of the Z_b and Z_c tetraquarks reveals that the isospin-1 B-O potentials are deeper in energy than the flavor-singlet B-O potentials for quarkonium hybrids. I wrote a paper explaining how the discovery of the $Z_c(3900)$ could be combined with lattice QCD calculations of the spectrum of charmonium hybrids to reveal the spectrum of charmonium tetraquarks. Langmack, Smith, and I also derived selection rules for hadronic transitions that could help narrow down the possible identifications of various XYZ mesons with the Born-Oppenheimer energy levels for hybrids and tetraquarks.

Dark Matter with Strong Self-interactions

The standard paradigm for dark matter is weakly interacting massive particles, whose self-interactions can be almost completely ignored. However there are some aspects of dark matter that provide hints of strong self-interactions at low-energy. One such hint is the apparent absence of cusps in the dark matter density at the cores of dwarf galaxies. This can be explained by dark matter particles having an energy-dependent cross section that is more than 12 orders of magnitude larger than the weak-interaction cross section when their relative velocity is about 10^{-4}. Cross sections that depend dramatically on the relative velocity can arise from the existence of an S-wave bound state very close to the threshold for a pair of dark matter particles. Hammer and I pointed out that such dark matter particles have universal behavior at low energy that is completely determined by the binding energy and width of the bound state. Laha and I studied the effects of the breakup of the universal bound state of two dark matter particles in collisions with nuclei in dark matter detectors. The occurence of this universal behavior in dark matter may be a long shot, but the fact that it is so predictive makes it worth exploring.

Publications since 2011

1. *Estimating the Production Rate of Loosely-bound Hadronic Molecules using Event Generators*,
   P. Artoisenet and Eric Braaten,
   Phys. Rev. D **83**, 014019 (2011) [arXiv:1007.2868].

2. *Universal Relations for Fermions with Large Scattering Length*,
   Eric Braaten,
   Lect. Notes Phys. **836**, 192-231 (2012) [arXiv:1008.2922].

3. *Universal Relations for Identical Bosons from 3-Body Physics*,
   Eric Braaten, DaekyoungKang, and L. Platter,
   Phys. Rev. Lett. **106**, 153005 (2011) [arXiv:1101.2854].

4. *Renormalization in the Three-body Problem with Resonant P-wave Interactions*,
   Eric Braaten, P. Hagen, H.-W. Hammer, and L. Platter,
   Phys. Rev. A **86**, 012711 (2012) [arXiv:1110.6829].

5. *Universal Relation for the Inelastic Two-Body Loss Rate*,
   Eric Braaten and H.-W. Hammer,
   J. Phys. B **46**, 215203 (2013) [arXiv:1302.5617]

6. *Universal Two-body Physics in Dark Matter near an S-wave Resonance*,
   Eric Braaten and H.-W. Hammer,
   Phys. Rev. D **88**, 063511 (2013) [arXiv:1303.4682].

7. *J/ψ Decay Channel of the X(3872) Charm Meson Molecule*,
   Eric Braaten and D. Kang,
   Phys. Rev. D **88** 014028 (2013) [arXiv:1305.5564].

8. *How the $Z_c(3900)$ Reveals the Spectra of Quarkonium Hybrid and Tetraquark Mesons*,
   Eric Braaten,
   Phys. Rev. Lett. **111**, 162003 (2013) [arXiv:1305.6905].

9. *Quarkonium at the Frontiers of High Energy Physics: A Snowmass White Paper*,
   G.T. Bodwin, Eric Braaten, E. Eichten, S.L. Olsen, T.K. Pedlar, and J.Russ,
   arXiv:1307.7425.

10. *Two-Body and Three-Body Contacts for Identical Bosons near Unitarity*,
    D. Hudson Smith, Eric Braaten, D. Kang, and L. Platter,
    Phys. Rev. Lett. **112**, 110402 (2014) [arXiv:1309.6922].

11. *Direct detection of dark matter in universal bound states*,
    Ranjan Laha and Eric Braaten,
    Phys. Rev. D **89**, 103510 (2014) [arXiv:1311.6386].

12. *J/ψ and Υ Polarization in Hadronic Production Processes*,
    Eric Braaten and J. Russ,
    arXiv:1401.7352.

13. *Selection Rules for Hadronic Transitions of XYZ Mesons*,
    Eric Braaten, Christian Langmack, and D. Hudson Smith,
    Phys. Rev. Lett. **112**, 222001 (2014) [arXiv:1401.7351].

14. *Born-Oppenheimer Approximation for the XYZ Mesons*,
    Eric Braaten, Christian Langmack, and D. Hudson Smith,
    arXiv:1402.0438.

Awards since 2011

Distinguished Alumni Fellow Award, May 2012
Department of Physics, University of Wisconsin–Madison

Simons Fellowship, 2014
Simons Foundation

3 Samir Mathur

My research program over the past several years has focused on resolving the black hole information paradox. This long standing paradox was noted by Stephen Hawking in 1974, who showed that under conventional assumptions about quantum gravity, the process of black hole formation and evaporation will violate the unitarity of quantum mechanics. Thus resolving this paradox will have to teach us something nontrivial about gravity and spacetime, and this in turn will be vital for understanding other fundamental problems like the physics of the early Universe.

Our work on this problem has led to the 'fuzzball proposal' for the interior structure of black holes. The crucial insight from the fuzzball proposal is that the effects of quantum gravity are not confined to the planck scale, which is very small (10^{-33} cm). Rather, when a large number of particles N are involved, the nonlocal quantum effects stretch over distances that are N^{α} times the planck length; here α is such that in black holes the effects reach all the way to the horizon, changing the black hole into a quantum 'fuzzball'.

Over the past few years we have made progress on several fronts, as described below.

The entropy of Rindler space and de Sitter space

It is known that black holes have an entropy given by the surface area of their horizon. But other spaces have horizons too, for example there is a horizon in de Sitter space. If we assign an entropy to such a horizon what would it mean? In a black hole, the entropy gave the number of possible internal states of the hole. But de Sitter space is *empty*, so what does its boundary area count?

This question was answered in the following way. In field theory we define a complete set of states as a set with the property $\sum_n |n\rangle\langle n| = I$. The microstates of black holes are fuzzballs, and it was argued that fuzzballs make a 'complete set of states for gravity'. de Sitter space can be divided across its horizon by the insertion of such a complete set, and then the entropy is given by the number of states that effectively appear in this sum. Concretely, this entropy counts the number of compact solutions of gravity with a positive Cosmological constant that end smoothly in set of KK monopoles before reaching the horizon.

Construction of microstates

It is crucial to understand the set of all fuzzball states, since they are the microstates of black holes. One way to categorize these states is through the dual CFT, where all states can be explicitly listed. A subset of the 3-charge D1-D5 -P CFT states are obtained by applying chiral algebra generators to 2-charge D1-D5 states. In a set of papers with Turton and with Lunin and Turton , we showed how such states can be constructed in the gravity description, both at the linear perturbation and fully nonlinear levels. This construction brings us closer to understanding the set of all black hole microstates.

Black hole complementarity

An important issue with black holes is: what does an observer feel as he falls through the black hole horizon? The fuzzball construction shows that spacetime ends at the horizon in a

stringy mess. Does this mean that an infalling observer will end his existence when he hits the horizon? We argued that there are two dual descriptions of the infall process: one where he gets absorbed into excitations of the fuzzball, and another where he seems to continue through. The underlying physics is similar to that of AdS/CFT duality: in one language an infalling quantum hits a collection of branes and gets absorbed in the process of exciting these branes. In another description the branes can be replaced by smooth AdS space, into which the quantum falls smoothly. The fuzzball construction provides the degrees of freedom at the horizon which are analogous to the branes in AdS/CFT, and the rest of the physics follows.

Over the past couple of years, Almheiri, Marolf, Polchinski and Sully put forth an argument that one could not have the kind of complementarity postulated by Susskind, where one observer sees that information is returned to infinity while another feels that the information falls into the hole. But the argument of thee authors did not take into account the basic tenet of 'fuzzball complementarily', where low energy ($E \sim T$) processes carry information out while $E \gg T$ processes natural to infalling observers have an approximate complementary description. In collaboration with postdoc David Turton, I explained how fuzzball complementarity evades the assumptions of the above mentioned argument against traditional complementarity.

Cosmology

The early Universe was a very dense place, much like the singularity at the center of a black hole. Since black hole microstates are fuzzballs, and we have understood much about fuzzball dynamics, one may ask if these ideas also extend to Cosmology. In recent work with Ali from Tufts University, I argued for a Universal equation of state at high energy densities. It was found that if we require the expression for the entropy $S(E, V)$ to be invariant user the dualities of string theory, then we get a unique expression, upto an overall constant of order unity. With this equation of state, we conjecture that tunneling into fuzzball states generates an 'expansive push' towards larger volumes of the Universe; this is a purely quantum effect arising from the large entropy of early Universe microstates. Such a push could be relevant for understanding inflation as well as the dark energy today.

Research Papers since 2011

1. **"An equation of state in the limit of high densities"**
   A. Masoumi and S. D. Mathur.
   arXiv:1406.5798 [hep-th]

2. **"Remnants, Fuzzballs or Wormholes?"**
   S. D. Mathur.
   arXiv:1406.0807 [hep-th]

3. **"Effect of the twist operator in the D1D5 CFT"**
Z. Carson, S. Hampton, S. D. Mathur and D. Turton.
arXiv:1405.0259 [hep-th]

4. **"What is the dual of two entangled CFTs?"**
S. D. Mathur.
arXiv:1402.6378 [hep-th]

5. **"Fuzzballs and black hole thermodynamics"**
S. D. Mathur.
arXiv:1401.4097 [hep-th]

6. **"Oscillating supertubes and neutral rotating black hole microstates"**
S. D. Mathur and D. Turton.
arXiv:1310.1354 [hep-th]
10.1007/JHEP04(2014)072
JHEP **1404**, 072 (2014)

7. **"What does strong subadditivity tell us about black holes?"**
S. D. Mathur.
arXiv:1309.6583 [hep-th]
10.1016/j.nuclphysbps.2014.04.003
Nucl. Phys. Proc. Suppl. **251-252**, 16 (2014)

8. **"What happens at the horizon?"**
S. D. Mathur.
arXiv:1308.2785 [hep-th]
10.1142/S0218271813410162
Int. J. Mod. Phys. D **22**, 1341016 (2013)

9. **"The flaw in the firewall argument"**
S. D. Mathur and D. Turton.
arXiv:1306.5488 [hep-th]
10.1016/j.nuclphysb.2014.05.012
Nucl. Phys. B **884**, 566 (2014)

10. **"A toy black hole S-matrix in the D1-D5 CFT"**
O. Lunin and S. D. Mathur.
arXiv:1211.5830 [hep-th]
10.1007/JHEP02(2013)083
JHEP **1302**, 083 (2013)

11. **"D1-D5-P microstates at the cap"**
S. Giusto, O. Lunin, S. D. Mathur and D. Turton.
arXiv:1211.0306 [hep-th]
10.1007/JHEP02(2013)050
JHEP **1302**, 050 (2013)

12. **"Comments on black holes I: The possibility of complementarity"**
S. D. Mathur and D. Turton.
arXiv:1208.2005 [hep-th]
10.1007/JHEP01(2014)034
JHEP **1401**, 034 (2014)

13. **"Adding momentum to supersymmetric geometries"**
O. Lunin, S. D. Mathur and D. Turton.
arXiv:1208.1770 [hep-th]
10.1016/j.nuclphysb.2012.11.017
Nucl. Phys. B **868**, 383 (2013)

14. **"Black holes and holography"**
S. D. Mathur.
arXiv:1207.5431 [hep-th]
10.1088/1742-6596/405/1/012005
J. Phys. Conf. Ser. **405**, 012005 (2012)

15. **"What can the information paradox tell us about the early Universe?"**
S. D. Mathur.
arXiv:1205.3140 [hep-th]
10.1142/S0218271812410027
Int. J. Mod. Phys. D **21**, 1241002 (2012)

16. **"Black Holes and Beyond"**
S. D. Mathur.
arXiv:1205.0776 [hep-th]
10.1016/j.aop.2012.05.001
Annals Phys. **327**, 2760 (2012)

17. **"Momentum-carrying waves on D1-D5 microstate geometries"**
S. D. Mathur and D. Turton.
arXiv:1202.6421 [hep-th]
10.1016/j.nuclphysb.2012.05.014
Nucl. Phys. B **862**, 764 (2012)

18. **"The information paradox: conflicts and resolutions"**
S. D. Mathur.
arXiv:1201.2079 [hep-th]
10.1007/s12043-012-0417-z
Pramana **79**, 1059 (2012)

19. **"Microstates at the boundary of AdS"**
S. D. Mathur and D. Turton.
arXiv:1112.6413 [hep-th]
10.1007/JHEP05(2012)014
JHEP **1205**, 014 (2012)

20. **"What the information paradox is not"**
S. D. Mathur.
arXiv:1108.0302 [hep-th]

21. **"Effective information loss outside the horizon"**
S. D. Mathur.
arXiv:1105.5616 [hep-th]
10.1007/s10714-011-1206-6, 10.1142/S0218271811020767
Gen. Rel. Grav. **43**, 2561 (2011), [Int. J. Mod. Phys. D **20**, 2881 (2011)] (2011)

22. **"Losing information outside the horizon"**
S. D. Mathur.
arXiv:1104.0612 [hep-th]

23. **"Correlations in Hawking radiation and the infall problem"**
S. D. Mathur and C. J. Plumberg.
arXiv:1101.4899 [hep-th]
10.1007/JHEP09(2011)093
JHEP **1109**, 093 (2011)

24. **"The Information paradox and the infall problem"**
S. D. Mathur.
arXiv:1012.2101 [hep-th]
10.1088/0264-9381/28/12/125010
Class. Quant. Grav. **28**, 125010 (2011)

Awards since 2011

- Fourth prize in Gravity Research Foundation Essay competition 2011
- Physics Department graduate course teaching award (2011)
- Physics Department under-graduate course teaching award (2011)
- Second prize in Gravity Research Foundation Essay competition 2012
- Third prize in Gravity Research Foundation Essay competition 2013
- Distinguished Scholar Award (Ohio State) 2014

4 Stuart Raby

My research in elementary particle physics focuses on physics beyond the Standard Model. In particular, I am one of the original proponents of the supersymmetric extension of the Standard Model. The so-called minimal supersymmetric standard model is now the new standard model of particle physics; which means to say it is the theory which is 1) the standard by which all other theories beyond the standard model are compared and 2) will be the first to be tested at the LHC. In addition, I am one of the originators of supersymmetric grand unified theories. At the moment, the unification of the three low energy gauge coupling constants is the only indicator of low energy supersymmetry in nature. I have also worked on obtaining fermion masses and mixing angles in self-consistent grand unified models and also in string theoretical constructions.

There are many good reasons to focus my research on supersymmetric models. In particular, let me describe what I believe are the virtues of supersymmetric grand unified theories [SUSY GUTs]. The following is a list of all the issues that SUSY GUTs either addresses directly or provides a framework for addressing

1) $M_Z << M_{GUT}$ "Natural"; 2) Explains Charge Quantization and family structure; 3) Predicts Gauge Coupling Unification*; 4) Predicts Yukawa Coupling Unification; 5) + Family Symmetry $\Longrightarrow$ Hierarchy of Fermion Masses; 6) Neutrino Masses via See - Saw scale $\sim 10^{-3} - 10^{-2}\ M_G$; 7) LSP – Dark Matter Candidate; 8) Baryogenesis via Leptogenesis; 9) SUSY Desert $\Longrightarrow$ LHC experiments probe physics O(M_{Planck}) scale; 10) SUSY GUTs are natural extension of the Standard Model

I have worked in three separate directions. These come under the categories of 1) supersymmetric model building; 2) the analysis of the consequences of these models for experiments at the LHC, at underground detectors looking for proton decay or neutrino oscillations, and at experiments analyzing the possible astrophysical consequences of these models and 3) string phenomenology.

1) Supersymmetric model building

In Refs. [1,2] we find a new discrete symmetry Z_4^R which is consistent with grand unification and solves several problems of the minimal supersymmetric standard model. We also obtain string theory models which realize our discrete symmetry. This symmetry can be considered to provide a natural understanding of the MSSM, i.e. by solving the mu problem, suppressing dimension 5 B and L violating operators and forbidding all R parity violating operators.

In Ref. [3], with my student Archana Anandakrishnan, we have written a paper on gauge mediated supersymmetry breaking in string models and the effect on gauge coupling unification. We show that string models can in general have more than one source of SUSY breaking, in particular gravity, gauge mediated and anomaly mediation can occur simultaneously, providing a low energy spectrum consistent with gauge coupling unification.

In Ref. [4] we have found several different discrete R symmetries consistent with grand unification, which provide phenomenologically acceptable low energy theories. Several naturally define the MSSM, while others can give either the NMSSM or an axion solution to the strong CP problem.

In Ref. [5] my student, Archana Anandakrishnan, and I study an SU(6) orbifold GUT

defined on Minkowski space, times the two dimensional orbifold with the topology of RP^2. We discuss gauge coupling unification when we break SU(6) down to the Standard Model via a combination of a Z_2 parity and a "non-local" Wilson line. The motivation for this work was to find an application to string theory constructions with effective SU(6) orbifold GUTs. The model is consistent with precise gauge coupling unification at the GUT scale.

I have worked on fermion masses and mixing angles in the context of supersymmetric GUTs with family symmetries. In two papers with Blazek and Dermisek (Phys. Rev. Lett. **88**, 111804 (2002) [hep-ph/0107 097]; Phys. Rev. D **65**, 115004 (2002) [hep-ph/0201081]) we showed that an SO(10) SUSY GUT with the minimal Yukawa coupling for the third family constrains SUSY parameter space and makes significant predictions for squark , slepton and gaugino masses. This is due to the fact that the bottom and tau masses receive large radiative corrections proportional to $\tan\beta$ which depends on the supersymmetric spectrum. Thus, in order to fit the top, bottom and tau masses the boundary conditions of soft SUSY breaking parameters at the GUT scale are severely constrained. Recently we have re-analyzed the model, Ref. [6] with emphasis on comparing to the latest bounds from the LHC, in particular, including a Higgs with mass ~ 125 GeV. We extend the upper bound on the universal scalar mass parameter $m_{16} \leq 30$ TeV and find good fits with an upper bound on the gluino mass, $m_{\tilde{g}} \leq q2$ TeV. We have also performed a three family global χ^2 analysis based on a three family model for fermion masses by Dermisek and myself (Phys. Lett. B **622**, 327 (2005) [hep-ph/ 0507045]). This model was also extensively studied by Albrecht et al. (JHEP **0710**, 055 (2007) [arXiv:0707.3954 [hep-ph]]). The reason to consider the extension of the model is that it fits all fermion masses and mixing angles quite well $\chi^2/dof \approx 2$, is extremely predictive and is still consistent with LHC and flavor bounds. The global χ^2 fit uses the code Maton (written by Radovan Dermisek, Indiana University and modified by my student, Archana, and Akin Win gerter, postdoc at Grenoble) which starts with GUT scale parameters, renormalizes down to the weak scale and then evaluates the particle spectrum with output in the SLHA format. The major modification of the code integrates out the first two family of squarks and sleptons at the scale m_{16}. For the Higgs mass calculation this is accomplished using the code of P. Slavich. Flavor observables are then calculated using SUSYFLAVOR and SuperISO, while thermal dark matter abundance is calculated using MicrOmegas. Finally at the weak scale electroweak symmetry is spontaneously broken self-consistently and a χ^2 function is evaluated with 24 arbitrary parameters (22 defined at the GUT scale and $\mu, \tan\beta$ defined a the weak scale) to fit 36 low energy observables. The χ^2 function is then minimized using the CERN code, MINUIT.

We are also interested in testing different soft SUSY breaking boundary conditions at the GUT scale which may be consistent with Yukawa unification. In the paper Ref. [7] we found boundary conditions with universal scalar masses but non-universal gaugino masses which fits the third family low energy data. The gaugino mass are described by effective "mirage" mediation boundary conditions. The low energy SUSY spectrum is quite interesting with degenerate chargino-neutralino masses. A gain this model is not obviously excluded by LHC data. What I mean by this is explained in the next section.

2) Phenomenology

We are now performing a detailed analysis of the consequences of our models for LHC physics. LHC SUSY searches performed by either ATLAS or CMS use benchmark points based on the CMSSM or simplified models to test for SUSY and put constraints on the SUSY spectrum. The LHC is particularly sensitive to observing colored particles such as gluinos or squarks. It is less sensitive to charginos or sleptons. Our models are certainly not part

of the CMSSM parameter space. And so we cannot trust limits based on these benchmark points. In addition our models have the property that the third family of squarks and sleptons are lighter than the first two families. This is what makes them consistent with flavor bounds. Thus they are closer to simplified models which assume $m_{squark} \gg m_{\ tildeg}$ and 100% branching ratios for the decays $\tilde{g} \to t\,\bar{t}\,\tilde{\chi}_1^0$ or $\tilde{g} \to b\,\bar{b}\,\tilde{\chi}_1^0$. Limits on the gluino mass assuming these simplified models is now in the range 1 - 1.2 TeV from CMS and ATLAS analyses with the best bounds coming from hadronic plus missing energy searches. However we have evaluated the decay branching ratios in our models using SDecay and again they are very much different than these simplified models. Thus, in collaboration with Akin Wingerter (postdoc at Laboratoire de Physique Subatomique et de Cosmologie, Grenoble, France), and my students, Archana Anandakrishnan and B . Charles Bryant, we have evaluated the signals for the benchmark points of Refs. [8,9] for 7, 8 and future 13 TeV LHC studies. We use the output of the code Maton discussed above. We use SDecay to calculate decay branching ratios and Prospino to evaluate the NLO sparticle production cross-sections which are given in terms of the tree level cross-section times a multiplicative K factor. We then use Pythia to evaluate the SUSY production and decay probabilities. Since Pythia only uses tree level sparticle production cross-sections, we multiply the output by the relevant K factor. These results are then input into the detector simulator Delphes which provides output with the correct acceptances and efficiencies more or less consistent with CMS. The output from Delphes is a root file which contains all the data. We then compare this data with CMS analyses which provide the number of allowed signal events at 95% CL in specific channels defined by the appropriate cuts. We find gluino masses less than a TeV are excluded by CMS data for these benchmark points, Ref. [8]. Similar analyses testing Yukawa unified models at the LHC have been performed previously in the literature, see JHEP **1002**, 055 (2010) [arXiv:0911.4739 [hep-ph]]. The upper bound on the gluino mass in our analysis has been increased by allowing for larger value s of m_{16}. Preliminary results suggest that due to the many decay channels available for our gluinos, in particular a significant decay branching ratio into a gluon-neutralino final state, gluinos with mass of order 1 TeV and greater are not excluded by CMS data for hadronic jets plus missing energy. Archana has given a talk at the pre-Snowmass meeting on the Energy Frontier at the KITP and we have submitted a contribution to Snowmass, Ref. [9]. Finally in Ref. [10] with Archana and Charles, we have used ATLAS and CMS 7 and 8 TeV data to place a lower bound on the gluino mass in the context of general models consistent with Yukawa unification. We find that in most cases the gluino must be heavier than 1.2 TeV, with the exception of models with compressed gaugino spectra. In this latter case this data does not provide any limits. We are now performing a more general LHC analysis of models with degenerate chargino - neutralino pairs, such as is present in anomaly mediated SUSY breaking or light Higgsino models. In particular, with Linda Carpenter and Archana Anandakrishnan, we are analyzing events with mono-photons, mono-Zs or mono-jets.

3) String Phenomenology

Since 2003 I have been working in the area of string phenomenology. That is to say, attempting to find the MSSM in the string landscape. The first papers with my collaborators T. Kobayashi and R.J. Zhang (Phys. Lett. B **593**, 262 (2004)[hep-ph/0 403065]; Nucl. Phys. B **704**, 3 (2005) [hep-ph/0409098]), focused on orbifold contructions in the $E(8) \times E(8)$ heterotic string. We showed how one can can obtain the ultra-violet completion of six dimensional orbifold GUT field theories in the 10 dimensional heterotic string. This work lead to the construction by Buchmüller et al. (Phys. Rev. Lett. **96**, 121602 (2006) [hep-ph/0511035]) of three family heterotic orbifold models. Then with my collaborators, Lebedev

et al. we wrote a series of papers on searches for the MSSM in the heterotic landscape, (Phys. Lett. B **645**, 88 (2007)[hep-th/0611095]; Phys. Rev. Lett. **98**, 181602 (2007)[hep-th/0611203]; Phys. Rev. D **77**, 046013 (2008)[arXiv:0708 .2691 [hep-th]]). We were quite successful, obtaining several hundred models which are very much MSSM-like and, in addition, a class of 15 string models which we believe are the most phenomenologically acceptable models found so far in the string theory literature. We studied two of these models in great detail and they are both quite realistic in all respects. In a subsequent paper with Dundee and Westphal (Phys. Rev. D **82**, 126002 (2010) [arXiv:1002.1081 [hep-th]]), we investigated the conditions necessary for stabilizing the many moduli of the theory and also discuss the spontaneous breaking of supersymmetry and the resultant super particle spectrum. Finally in a paper with Bobkov et al. (JHEP **1012**, 056 (2010)[arXiv:100 3.1982 [hep-th]]), we studied the same issue but in Type IIB string models.

In collaboration with Joseph Marsano (University of Chicago), Herb Clemens and Hsian-Hua Tseng (Dept. Math., OSU), and Tony Pantev (Dept. Math., University of Pennsylvania), Ref. [11], we obtain a complete global F theory construction of the MSSM with Wilson line breaking of an $SU(5)$ GUT. This is the first such construction in the literature. The model has one fatal problem in that we show that we obtain massless vector-like exotics which unfortunately destroy gauge coupling unification. Otherwise, the model has three families of quarks and leptons, the Standard Model gauge structure and four pairs of Higgs doublets at the massless level. We showed that the massless vector-like exotics sitting in the coset of a chiral adjoint of $SU(5)/[SU(3) \times SU(2) \times U(1)]$ will always be present using Wilson line breaking of $SU(5)$. This is not true for the Heterotic string, thus suggesting that a Wilson line in the Heterotic string is NOT dual to a Wilson line on the F theory side. Along with my collaborators, Herb Clemens, Hsian-Hua Tseng and Emanuele Macri (Dept. Math., Ohio State University), Tony Pantev (Dept. Math., U. Pennsylvania) and Sakura Schafer-Nameki (Dept. Math., Kings College, London) we are looking for the F theory dual of Heterotic models constructed by Donagi et al. (JHEP **0506**, 070 (2005) [hep-th/0411156]).

Publications since 2011

1. H. M. Lee, S. Raby, M. Ratz, G. G. Ross, R. Schieren, K. Schmidt-Hoberg and P. K. S. Vaudrevange, "A unique Z_4^R symmetry for the MSSM," Phys. Lett. B **694**, 491 (2011) [arXiv:1009.0905 [hep-ph]].

2. R. Kappl, B. Petersen, S. Raby, M. Ratz, R. Schieren and P. K. S. Vaudrevange, "String-Derived MSSM Vacua with Residual R Symmetries," Nucl. Phys. B **847**, 325 (2011) [arXiv:1012.4574 [hep-th]].

3. A. Anandakrishnan and S. Raby, "Gauge Coupling Unification in Heterotic String Models with Gauge Mediated SUSY Breaking," Phys. Rev. D **83**, 075008 (2011) [arXiv:1101.1976 [hep-ph]].

4. H. M. Lee, S. Raby, M. Ratz, G. G. Ross, R. Schieren, K. Schmidt-Hoberg and P. K. S. Vaudrevange , "Discrete R symmetries for the MSSM and its singlet extensions," Nucl. Phys. B **850**, 1 (2011) [arXiv:1102.3595 [hep-ph]].

5. A. Anandakrishnan and S. Raby, "SU(6) GUT Breaking on a Projective Plane," Nucl. Phys. B **868**, 627 (2013) [arXiv:1205.1228 [hep-ph]].

6. A. Anandakrishnan, S. Raby and A. Wingerter, "Yukawa Unification Predictions for the LHC," Phys. Rev. D **87**, 055005 (2013) [arXiv:1212.0542 [hep-ph]].

7. A. Anandakrishnan and S. Raby, "Yukawa Unification Predictions with effective "Mirage" Mediation," Phys. Rev. Lett. **111**, 21, 211801 (2013) [arXiv:1303.5125 [hep-ph]].

8. A. Anandakrishnan, B. C. Bryant, S. Raby and A. Wingerter, "LHC Phenomenology of SO(10) Models with Yukawa Unification," Phys. Rev. D **88**, 075002 (2013) [arXiv:1307.7723 [hep-ph]].

9. A. Anandakrishnan, B. C. Bryant, S. Raby and A. Wingerter, "Gluino bounds: Simplified Models vs a Particular SO(10) Model (A Snowmass white paper)," [arXiv:1308.2232 [hep-ph]].

10. A. Anandakrishnan, B. C. Bryant and S. Raby, "LHC Phenomenology of SO(10) Models with Yukawa Unification II," [arXiv:1404.5628 [hep-ph]].

11. J. Marsano, H. Clemens, T. Pantev, S. Raby and H. -H. Tseng, "A Global SU(5) F-theory model with Wilson line breaking," JHEP **1301**, 150 (2013) [arXiv:1206.6132 [hep-th]].

5 Junko Shigemitsu

During the past couple of years I have worked with postdocs Heechang Na (OSU 2008-2011), Chris Bouchard (OSU 2011-2014), Chris Monahan (William & Mary) and with senior collaborators Peter Lepage (Cornell), Christine Davies (Glasgow) and Ron Horgan (Cambridge) on D, B and B_s meson semileptonic and leptonic decays, on B meson rare decays and on Neutral B meson mixing parameters. The goal of our collaboration (the HPQCD collaboration) is to provide experimentalists and flavor phenomenologists with crucial non-perturbative QCD input necessary for testing the Standard Model (SM). Precision Flavor Physics is a very viable approach to searching for Beyond the Standard Model Physics. To do so, however, requires accurate Standard Model predictions which can be tested against precise experimental data. The accuracy of Lattice QCD calculations has improved to the point that lattice results are now playing an important role in these tests of the Standard Model and the calculations by the HPQCD collaboration of decay constants, form factors and mixing parameters are having impact.

$|V_{cd}|$ from D Meson Semileptonic and Leptonic Decays

In 2010 we published new results on the D meson semileptonic decay, $D \to K, l\nu$, (H.Na *et al.*; Phys.Rev **D82**, 114506 (2010)) that reduced the errors on $f_+^{D\to K,l\nu}(0)$ by a factor of four to 2.5%. This significant reduction in errors was made possible due to the use of the "Highly Improved Staggered Quark" (HISQ) action, developed by our collaboration, for both charm and light quarks. This HISQ action has very small discretization errors and allows for absolutely normalized currents. Furthermore during the past couple of years we have developed and implemented many novel data analysis tools. Combining our new result for $f_+^{D\to K,l\nu}(0)$ with experimental input from CLEO-c and BaBar we determined the CKM matrix element,

$$|V_{cs}| = 0.961(11)(24)$$

where the first error is from experiment and the second from theory.

As the next project we focused on another CKM matrix element $|V_{cd}|$ using both semileptonic and leptonic D meson decays. First we completed and published a state-of-the-art calculation of the form factor $f_+^{D\to\pi,l\nu}(q^2 = 0)$ with a better than factor of two smaller error than in previous lattice determinations [2]. Combining with experimental input from CLEO-c we extracted,

$$|V_{cd}|_{semilept.} = 0.225(6)_{exp}(10)_{lat}.$$

In a more recent paper [5] we updated HPQCD's value for the D meson decay constant,

$$f_D = 208.3(3.4)\text{MeV},$$

and used this, together with branching fraction data from CLEO-c to extract,

$$|V_{cd}|_{leptonic} = 0.223(10)_{exp}(4)_{lat},$$

in excellent agreement with $|V_{cd}|_{semilept.}$. Both semileptonic and leptonic decay determinations of $|V_{cd}|$ agree well with the PDG value based on neutrino scattering of $|V_{cd}|_{neutrino} =$

0.230(11). The fact that three independent determinations, each based on very diferent theory and experimental inputs, agree with each other is a nontrivial consistency check on the Standard Model.

B and B_s Meson Decay Constants with NRQCD Bottom and HISQ Light/Strange Quarks

There is currently, within the Standard Model, some tension between results for ϵ_K, $\sin(2\beta)$, $|V_{ub}|$ and the branching fraction $\mathcal{B}(B^+ \to \tau^+\nu_\tau)$. The B meson decay constant f_B plays an important role in several of these processes. In one approach, phenomenologists do fits to precision electroweak data in such a way so that f_B is a fit output that can be compared with direct predictions from QCD. This way one can check for consistency between the electroweak data and the SM. There are, hence, strong incentives to calculate f_B via lattice QCD methods as accurately as possible.

In 2012 we completed a new calculation of f_B and f_{B_s} using NRQCD bottom quarks and HISQ strange and light quarks [4]. We find,

$$f_B = 191(9)\text{MeV}, \quad f_{B_s} = 228(10)\text{MeV}, \quad f_{B_s}/f_B = 1.188(18).$$

We also combined f_{B_s}/f_B with a recent very precise calculation of f_{B_s} based on HISQ heavy quarks and find,

$$\left[\frac{f_{B_s}}{f_B}\right]^{-1}_{NRQCD} \times f_{B_s}^{(HISQ)} \equiv f_B = 189(4)\text{MeV}.$$

This represents the most precise f_B available today and provides an important ingredient in Standard Model predictions for processes such as $\mathcal{B}(B^+ \to \tau^+\nu_\tau)$. The decay constant f_{B_s}, on the other hand, is crucial for Standard Model predictions for $\mathcal{B}(B_s -> \mu^+\mu^-)$. In reference [7] we updated the B and B_s decay constant results using simulations on configurations that included $N_f = 2+1+1$ (up, down, strange, charm) sea quarks and found decay constants very consistent with the above numbers, that were all based on $N_f = 2+1$ configurations.

The B Meson Rare Decays

The rare decay $B \to Kl^+l^-$ involves the $b \to s$ flavor changing neutral current process and hence does not occur at tree-level in the Standard Model. It goes through box or penguin diagrams and provides a sensitive probe for New Physics. Experimentalists (Belle, BaBar, CDF, LHCb) are collecting more and more data on this decay and comparisons with accurate Standard Model predictions have become important. Three form factors are needed to parametrize the decay rates. In addition to the vector and scalar form factors $f_+(q^2)$ and $f_0(q^2)$, one needs the tensor form factor $f_T(q^2)$. HPQCD recently published the first unquenched lattice determinations of these three form factors [8] [9]. We calculated Standard Model predictions for differential decay rates as functions of q^2 and compared with experimental branching fraction measurements from Belle, BaBar, CDF and LHCb. Agreement was found within current experimental and theory errors. By adjusting appropriate Wilson coefficients, these same form factors can be used by phenomenologists to predict decay rates in many other theories as well that go beyond the Standard Model.

Operator Matching

Calculations of hadronic matrix elements relevant to B meson semileptonic and leptonic decays require matching of the lattice heavy-light currents used in the simulations to their continuum QCD counter parts. This step is particularly cumbersome when using effective actions such as NRQCD for b-quarks and highly improved relativistic actions such as HISQ for charm and lighter quarks. In fact, the HISQ action is so complicated so that it is not practical to try and write down Feynman rules for this action. Instead, lattice perturbation theory is carried out using socalled "automated perturbation theory" computer codes developed by the HPQCD collaboration. We recently completed a project to carry out one-loop matching of NRQCD/HISQ currents for both massless and massive HISQ quarks [6]. These operator matching results were indespensable in the above B and B_s meson decay constant and rare decay projects.

Publications since 2011

Refereed articles :

1. "Precise B, B_s and B_c meson spectroscopy from full lattice QCD";
   E. B. Gregory, C. T. H. Davies, I. D. Kendall, J. Koponen, K. Wong, E. Follana, E. Gamiz, G. P. Lepage, E. H. Mueller, H. Na, and J. Shigemitsu, Phys. Rev. **D83**, 014506 (2011).

2. "$D \to \pi, l\nu$ Semileptonic Decays, $|V_{cd}|$ and 2^{nd} Row Unitarity from La ttice QCD";
   H. Na, C. T. H. Davies, E. Follana, J. Koponen, G. P. Lepage and J. Shigemitsu, Phys. Rev. D **84**, 114505 (2011) [arXiv:1109.1501 [hep-lat]].

3. "Fast Fits for Lattice QCD Correlators";
   K. Hornbostel, G. P. Lepage, C. T. H. Davies, R. J. Dowdall, H. Na and J. Shigemitsu, Phys. Rev. D **85**, 031504 (2012) [arXiv:1111.1363 [hep-lat]].

4. "The B and B_s Meson Decay Constants from Lattice QCD";
   H. Na, C. J. Monahan, C. T. H. Davies, R. Horgan, G. P. Lepage and J. Shigemitsu, Phys. Rev. D **86**, 034506 (2012) [arXiv:1202.4914 [hep-lat]].

5. "The $|V_{cd}|$ from D Meson Leptonic Decays";
   H. Na, C. T. H. Davies, E. Follana, G. P. Lepage and J. Shigemitsu, Phys. Rev. D **86**, 054510 (2012) [arXiv:1206.4936 [hep-lat]].

6. "Matching Lattice and Continuum Axial-Vector and Vector Currents with NRQCD and HISQ Quarks";
   C. J. Monahan, R. Horgan and J. Shigemitsu, Phys. Rev. D **87**, 034017 (2013) [arXiv:1211.6966 [hep-lat]].

7. "B-meson decay constants from improved lattice NRQCD and physical u, d, s and c sea quarks";
   R. J. Dowdall, C. T. H. Davies, R. R. Horgan, C. J. Monahan and J. Shigemitsu, Phys. Rev. Lett. 110:222003 (2013) [arXiv:1302.2644 [hep-lat]].

8. "Standard Model predictions for $B \to Kll$ with form factors from lattice QCD"; C. Bouchard, G. P. Lepage, C. Monahan, H. Na and J. Shigemitsu, Phys. Rev. Lett. 111:162002 (2013) [arXiv:1306.0434 [hep-ph]].

9. "The rare decay $B \to Kll$ form factors from lattice QCD"; C. Bouchard, G. P. Lepage, C. Monahan, H. Na and J. Shigemitsu, Phys. Rev. D **88**, 054509 (2013) [arXiv:1306.2384 [hep-lat]].

10. "The Shape of the $D \to K$ Semileptonic Form Factor from Full Lattice QCD and V_{cs}"; J. Koponen, C. T. H. Davies, G. C. Donald, E. Follana, G. P. Lepage, H. Na, J. Shigemitsu, [arXiv:1305.1462].

11. "$B_s \to Kl\nu$ Form Factors from Lattice QCD"; C. M. Bouchard, G. P. Lepage, C. Monahan, H. Na and J. Shigemitsu, [arXiv:1406.2279 [hep-lat]].

Proceedings articles :

12. "The D to K and D to pi semileptonic decay form factors from Lattice QCD"; J. Koponen *et al.* [The HPQCD Collaboration], arXiv:1111.0225 [hep-lat].

13. "Studies of B and B_s Meson Leptonic Decays with NRQCD Bottom and HISQ Light/Strange Quark s"; J. Shigemitsu, H. Na, C. Davies, R. Horgan, C. Monahan and P. Lepage, PoS **LATTICE 2011**, 291 (2011) [arXiv:1110.5783 [hep-lat]].

14. "Precise Determinations of the Decay Constants of B and D mesons"; H. Na, C. Monahan, C. Davies, E. Follana, R. Horgan, P. Lepage and J. Shigemitsu, PoS **LATTICE 2012**, 102 (2012) [arXiv:1212.0586 [hep-lat]].

15. "Matching heavy-light currents with NRQCD and HISQ quarks"; C. Monahan, C. Davies, R. Horgan, G. P. Lepage, H. Na and J. Shigemitsu, PoS **LATTICE 2012**, 125 (2012) [arXiv:1210.7016 [hep-lat]].

16. "Form factors for B and B_s semileptonic decays with NRQCD/HISQ quarks"; C. M. Bouchard, G. P. Lepage, C. J. Monahan, H. Na and J. Shigemitsu, PoS **LATTICE 2012**, 118 (2012) [arXiv:1210.6992 [hep-lat]].

17. " B and B_s semileptonic decay form factors with NRQCD/HISQ quarks"; C. M. Bouchard, G. P. Lepage, C. J. Monahan, H. Na and J. Shigemitsu, [arXiv:1310.3207 [hep-lat]].

18. "B, B_s, K and π weak matrix elements with physical light quarks"; R. J. Dowdall, C. T. H. Davies, R. Horgan, G. P. Lepage, C. McNeile, C. Monahan, J. Shigemitsu, PoS **LATTICE 2013**, 406 (2014) [arXiv:1309.4610 [hep-lat]].

Awards since 2011

1. The Ohio State University "Distinguished Scholar Award" (2011)

2. Society of Physics Students (Ohio State) "2014 Undergraduate Outstanding Teacher Award".

Final Report for the period 12/1/2010-4/30/2014

Task D/ATLAS

Grant DE-FG02-91ER40690

K.K. Gan
H. Kagan
R. Kass

Department of Physics
The Ohio State University
191 West Woodruff Avenue
Columbus, Ohio 43210

July, 2014

Overview of the Ohio State University ATLAS group

Introduction

This report summarizes the activities of The Ohio State University ATLAS/Task D group (P. I.s Gan, Kagan, and Kass) over the three year period of the grant. The three faculty members have been working as part of the same Task since 1990, first on CLEO, next on BaBar, and since 1998 on ATLAS. Over the years they have taken on major responsibilities for both hardware construction and physics analysis on all of their experiments. During the grant period their research efforts have been dedicated to the energy frontier as members of the ATLAS Experiment [1]. Here they played a critical role in the pixel detector's optical readout system [2], the beam condition monitor (BCM) [3], the beam loss monitor (BLM) [4], and the newly installed diamond beam monitor (DBM) [5]. The group contributed to several physics analyses projects based on diboson events (e.g. γZ, WZ, and ZZ) that measure standard model (SM) processes and allow for searches of signatures of beyond the SM physics. In addition, they led a search for lepton number violation in Z decays and measurements of di-muon production in the Υ energy region. A brief summary of their recent ATLAS accomplishments is given below.

Recent accomplishments

- Successful data taking with the pixel detector's optical links, diamond based BCM and BLM at 7 and 8 TeV center of mass energy and luminosity in excess of $7 \times 10^{33}\ \mathrm{cm}^{-2}\mathrm{s}^{-1}$.
- Fabrication and installation of new opto-boards for the Insertable B Layer (IBL) and new service quarter panel (nSQP) upgrades to the pixel detector.
- Fabrication and installation of the DBM.
- Operation of a Tier 3 computing facility consisting of 72 (4.2GHz) CPU's and 100 TB of disc storage to perform data analysis locally.
- Published results for the WZ and ZZ cross sections and anomalous triple gauge couplings (aTGC) from the 7 and 8 TeV data sets.
- Published a measurement of di-muon production in the Upsilon region.
- Published results of a search for narrow states decaying into γZ, including upper limits for Low Scale Technicolor particles using the 7 TeV data set and a search for Higgs$\rightarrow \gamma Z$ using both the 7 and 8 TeV data sets.
- Performed a search for anomalous $e\mu$ production through the decay $Z \rightarrow e\mu$.
- Awarded PhDs to three graduate students for their research on ATLAS.

1 The Ohio State University ATLAS Program Activities

Members of the Ohio State ATLAS group have vigorously pursued their interests in hadron collider physics. As collaborators on the LHC's ATLAS experiment [1] we designed, fabricated, and commissioned the on-detector optical links of the pixel detector [6] as well as the BCM [3] and BLM [4]. The ATLAS detector performed extremely well, as evidenced by the large data set we have accumulated (Fig. 1) and its large number of publications (>250) including the discovery of a Higgs particle [7]. Members of our group have played key roles in the detector's operation including one of our postdocs (J. Moss) as the Pixel Run Coordinator and two of our graduate students (M. Fisher, H. Merritt) as the BCM and BLM Run Coordinator. At OSU we constructed an ATLAS Tier 3 Facility to perform data analysis. This facility is allowed us to analyze the large ATLAS data sample as well as generate samples of simulated events.

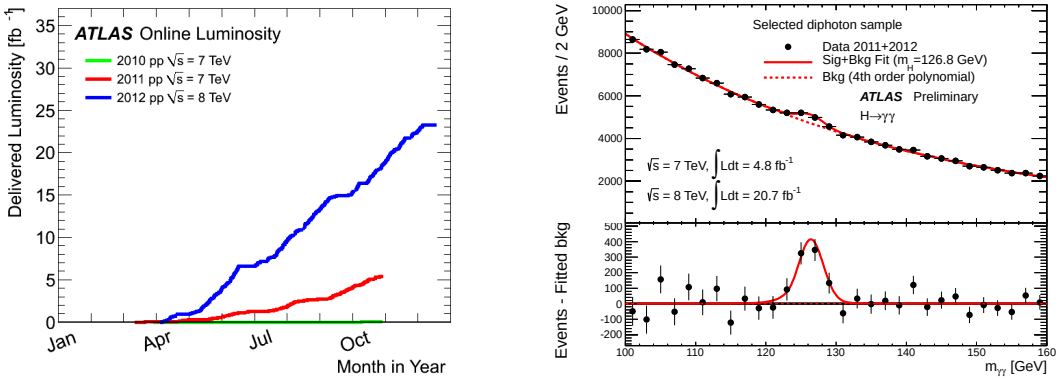

Figure 1: (left) ATLAS luminosity in 2010-12, and (right) Higgs$\longrightarrow \gamma\gamma$.

1.1 ATLAS Analysis Projects

1.1.1 Measurement of the WZ and ZZ Production Cross Sections and Triple Gauge Boson Couplings

The underlying structure of the SM electroweak interaction is the non-abelian $SU(2)_L \times U(1)_Y$ gauge group. Features like vector boson masses and their coupling to fermions have been precisely tested at LEP and the Tevatron. However triple gauge boson couplings (TGC) predicted by this theory have not yet been determined with the same precision. In the SM the TGC vertex is completely fixed and so a precise measurement of this vertex, through diboson production at the LHC, is essential to test the high energy behavior of electroweak interactions and to probe for possible new physics in the bosonic sector.

1.1.1.1 Measurement of the WZ Production Cross Sections and Triple Gauge Boson Couplings Graduate student, A. Nagarkar, analyzed WZ events in the 4.64b^{-1} of data collected at $\sqrt{s} = 7$ TeV. He measured the WZ production cross section and set limits on aTGCs. The results have been published in [8]. The WZ analysis formed the basis of Nagarkar's dissertation (Adviser K. K. Gan) and he graduated in FY13.

1.1.1.2 Measurement of the ZZ Production Cross Section and Triple Gauge Boson Couplings The $pp \to ZZX$ process is important both as a study of electroweak gauge symmetry of the SM as well as a background to Higgs searches. The $ZZ^* \to 4l$ channel is considered to be the Higgs golden channel as this final state has almost negligible background. However, this is a challenging final state to observe as $pp \to ZZ$ has the lowest cross section of any diboson final state and the four lepton decay only accounts for 0.5% of the decays.

Figure 2 shows the leading-order Feynman diagrams for ZZ^* production from $q\overline{q}$ and gg initial states. In the SM, the ZZZ and ZZ neutral triple gauge boson couplings are absent. Therefore measurements of these anomalous couplings (aTGCs) provide a sensitive test of the $SU(2)_L \times U(1)_\gamma$ gauge structure of the SM. Non-zero aTGCs would indicate the presence of new physics. In many models non-zero values of ZZZ and ZZ couplings would increase the ZZ cross section at high ZZ invariant mass and Z boson transverse momentum.

In Figure 3 (left) the invariant mass of the 7 TeV Z candidates passing all other analysis cuts is displayed. A clear $pp \to ZZX$ signal is present. The fiducial cross-section was measured to be $25.4^{+3.3}_{-3.0}(stat)^{1.2}_{1.0}(syst) \pm 0.4(lumi)$ fb for the ZZ final state and $29.8^{+3.8}_{-3.5}(stat)^{+1.7}_{-1.5}(syst) \pm 0.5(lumi)$ fb, for the ZZ^* final state. The total cross section for on-shell ZZ production has been determined to be $\sigma^{tot}_{ZZ} = 6.7 \pm 0.7(stat) \pm 0.4(syst) \pm 0.1(lumi)$ pb when combined with $ZZ \to \ell^+\ell^-\nu\overline{\nu}$. This is in agreement with the SM expectation of $5.89^{+0.22}_{-0.18}$ pb calculated at the next to leading order in QCD. There is no evidence for aTGCs and the limits set from the 7 TeV analysis are summarized in Fig. 4. The analysis is described in the ATLAS conference note ATL-COM-PHYS-2012-185.

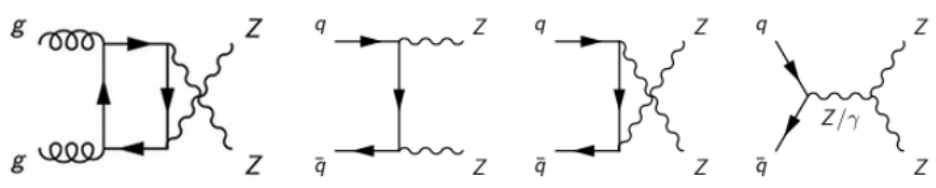

Figure 2: The Feynman diagrams for ZZ production through the $q\overline{q}$ and gg initial state. The s-channel diagram, on the right, contains the ZZZ neutral TGC vertex absent in the SM.

A similar analysis using the data collected during the run at $\sqrt{s} = 8$ TeV has been performed. The invariant mass distribution of the candidate Z's is shown in Fig. 3 (right). As shown in Table 1 a total of 305 ZZ candidate events were found in the 8 TeV data set which has an integrated luminosity of 20.4 fb^{-1}. The ZZ cross-section is measured to be

$$\sigma^{total}_{ZZ} = 7.1^{+0.5}_{-0.4}(stat.) \pm 0.3(syst.) \pm 0.2(lumi.)\text{pb}$$

in agreement with the SM prediction of $7.2^{+0.3}_{-0.2}$ pb. The analysis is described in the ATLAS conference note ATLAS-CONF-2013-020. There are four contributing TGCs: $f^\gamma_4, f^Z_4, f^\gamma_5$ and f^Z_5. The TGC limits set by ATLAS at center-of-mass energies of 7 and 8 TeV are compared to limits set at the Tevatron as shown in Fig. 4.

The PhD thesis topic of H. Merritt (Adviser R. Kass) was a measurement of the ZZ production cross section and aTGC limits using the entire 8 TeV data set.

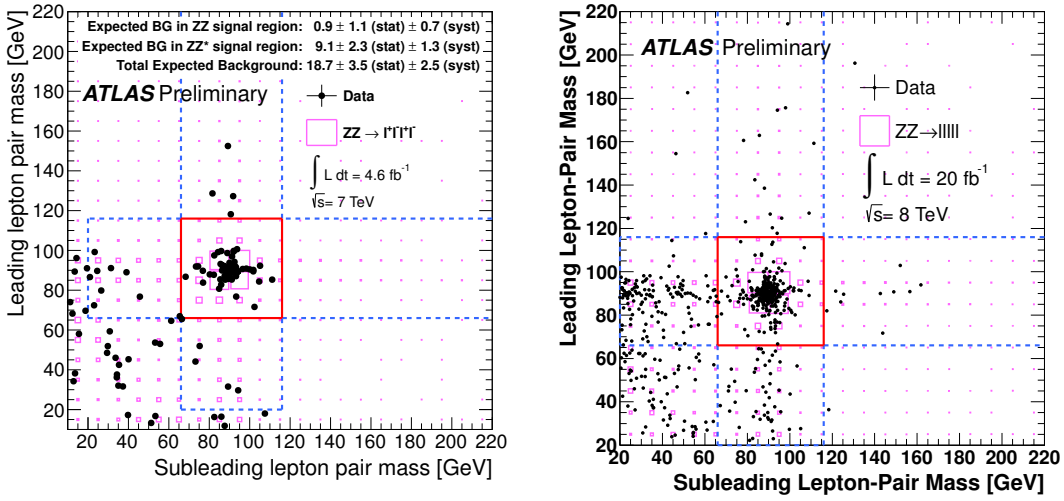

Figure 3: The mass of the leading lepton pair versus the mass of the subleading lepton pair for the 7 TeV (left) and 8 TeV (right) data samples. The events observed in the data are shown as solid circles and the $Z \rightarrow 4l$ signal prediction from simulation as boxes. The region enclosed by the solid red box (dashed blue boxes) indicates the signal region defined by the requirements on the lepton-pair masses for ZZ (ZZ^*) events, as defined in the text.

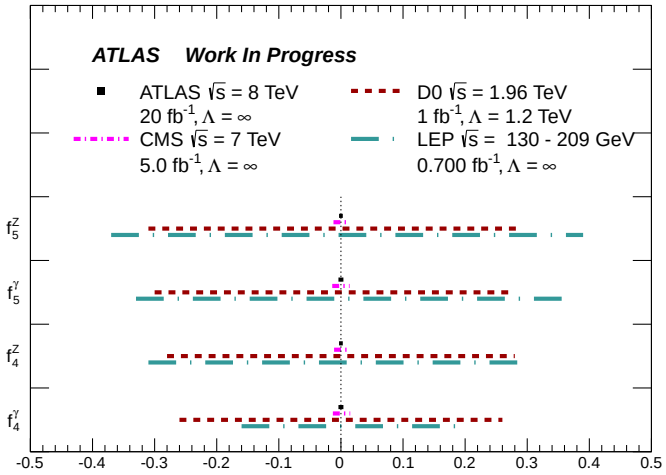

Figure 4: The 95% CLs on the aTGC in ZZ production from ATLAS, LEP, and Tevatron experiments. Luminosities, centre-of-mass energy and cut-off Λ for each experiment are shown.

Final state	$e^+e^-e^+e^-$	$\mu^+\mu^-\mu^+\mu^-$	$e^+e^-\mu^+\mu^-$	$\ell^+\ell^-\ell'^+\ell'^-$
Observed	62	85	158	305
Signal (MC)	59.5±4.0	90.2±2.7	142.7±5.6	292.5±10.6
Background	10.0±1.8±1.4	1.1±1.4±0.5	9.3±2.1±3.1	20.4±2.9±5.0

Table 1: Summary of observed events, expected signal and background contributions in all four-lepton channels, after applying the ZZ selection criteria.

1.1.2 Study of Low Mass Di-muon Pairs

There are many interesting physics processes around the Υ mass region, for example understanding quarkonium production in high energy pp collisions or searching for the production of new resonances. The di-muon final state is the golden channel for these studies.

The measurement of the Υ meson production cross-sections has been published [9]. The main analyzer and editor of this paper was OSU postdoc Yi Yang. Here the differential cross-sections of $\Upsilon(1,\ 2,\ 3S)$ mesons were measured at $\sqrt{s} = 7$ TeV using 1.8 fb^{-1} of data in fine p_T and rapidity intervals. We also measured the relative production rates of the excited states, $\Upsilon(2S)$ and $\Upsilon(3S)$, to the $\Upsilon(1S)$ state. The measurements were compared to theoretical calculations, the Color Singlet Mechanism (CSM) [10] in next-to-next-to-leading-order calculation (NNLO*CSM) and the Color Evaporation Model (CEM) [11]. The results provide important information for understanding quarkonium hadroproduction.

An extremely important and interesting topic being pursued is a search for a low mass CP-odd Higgs particle (a_1) decaying into di-muons. Next-to-Minimal SUSY provides an elegant solution of the μ-term problem and also predicts seven Higgs bosons. The mass interval being searched, 6-8 GeV, is one where B factory experiments have very little sensitivity. The analysis currently uses 4.3 fb^{-1} of 7 TeV data to optimize the signal selections for the 8 TeV data set (17.2 fb^{-1}). Figure 5 shows the expected limit[1] extrapolated from the 7 TeV data.

1.1.3 Search for Lepton Flavor Violating Decay $Z \to e\mu$

The LHC has already produced $100\times$ the number of Zs compared to LEP. This allows for a more sensitive search for the lepton flavor violating decay $Z \to e\mu$. We used data collected at 7 TeV to optimize the selection criteria for the search with the larger 8 TeV data set. There are several features in the analysis that greatly simplify the search. For example, the background is estimated from the data by fitting the observed $e\mu$ mass spectrum instead of using MC simulations and the number of $Z \to e\mu$ candidates observed in the data is normalized to the observed number of $Z \to ee$ and $\mu\mu$ candidates, resulting in the cancellation of most of the systematic errors. The above strategy allows us to impose stringent requirements on the maximum transverse momentum of hadronic jets and missing transverse energy of each event in order to suppress the enormous $Z \to \tau\tau$, $t\bar{t}$ and WW backgrounds. This analysis is in its final stages and we expect a significant improvement over the previous limit, 1.7×10^{-6}, set by OPAL at LEP [13].

[1] In this and other searches mentioned in this proposal we use the CLs method [12].

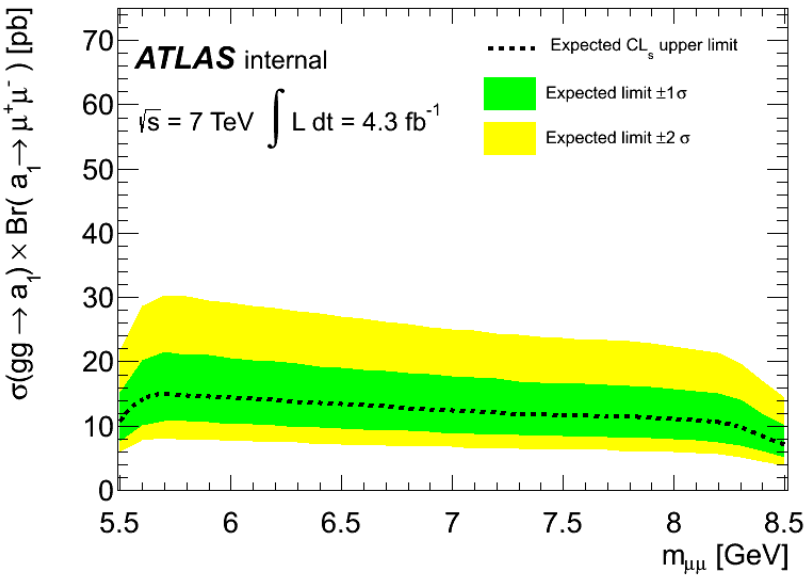

Figure 5: Expected upper limits on a_1 production cross section times branching fraction.

1.1.4 Search for Technicolor Particles and Higgs Boson Decaying into γZ

The SM has well defined predictions for all di-boson production cross sections. In this sense γZ production is similar to WZ and ZZ production. Using the small 2010 data set ATLAS measured the production cross section of a final state containing photon and a Z (CERN-PH-EP-2011-079). Our graduate student, M. Fisher, continued this analysis using 4.7 fb^{-1} of 7 TeV data. The cross section for γZ, where the Z decays into electrons (muons) was measured to be $1.26 \pm 0.07 \pm 0.07$ ($1.24 \pm 0.07 \pm 0.11$) pb, where the first error is due to statistics and the second due to systematics. The measurements agree with the SM expectation of 1.22 ± 0.05 pb.

A popular model to explain electro-weak symmetry breaking is Technicolor. Here a new QCD-like force is responsible for breaking the electro-weak symmetry. In a particular model known as Low Scale Technicolor (LSTC) [14, 15] bound states with masses in the several hundred GeV range can be produced in high energy pp collisions. These states (ρ_T, ω_T) can then decay into γZ. The width of these states is expected to be narrow. We have performed a detailed search for such particles decaying into γZ in the mass range 200-500 GeV using the 7 TeV data set. The 95% CL upper limits were determined using the standard ATLAS CL_s method. Figure 6 shows the exclusion range for this analysis. This work formed the basis of M. Fisher's Ph. D. dissertation (Adviser H. Kagan).

The decay $H \to Z\gamma$ is one of its cleanest modes, as there are no missing particles in the final state and only three particles to detect if the $Z \to l^+l^-$ mode is used. In the SM the branching fraction for $H \to Z\gamma$ with m_{Higgs} = 125 GeV is $\mathcal{B}(H \to Z\gamma) = 1.54 \times 10^{-3}$ (Fig. 7).

The search for the SM Higgs boson in $Z\gamma$ final state was done in the mass range between 120 and 150 GeV. The result of the search for the SM Higgs is shown in Fig. 7 as an exclusion limit for the SM Higgs cross-section times branching fraction as a function of mass. For a 125.5 GeV Higgs the observed 95% CL limit is 11$\times$ the SM Higgs cross-section. The results of this analysis were published in [16].

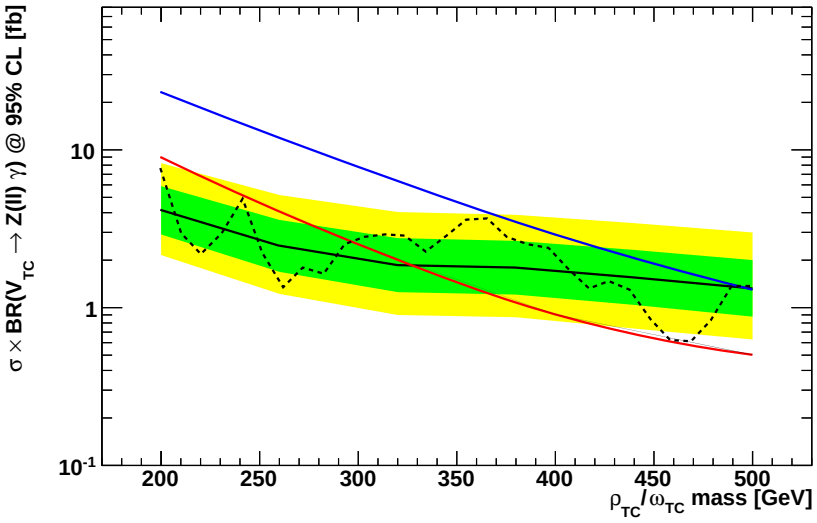

Figure 6: Upper limits on the LSTC rate as a function of mass. The solid black line is the expected limit, the yellow and green band are the 1 and 2 σ errors. The dashed line is the observed limit with the 7 TeV dataset. The blue line is the theoretical cross section used in the ATLAS search. The red line is for the parameters suggested by K. Lane [14].

1.2 OSU ATLAS Hardware Projects

The OSU group had major responsibilities in two detector systems, the optical readout of the pixel detector and three beam monitoring devices that use CVD diamond as the sensor material (BCM, BLM, and DBM). We briefly describe these efforts below.

1.2.1 Optical Links of ATLAS Pixel Detector

The OSU/ATLAS group led the design, prototyping, and production of the on-detector optical modules (opto-boards[2]) for the pixel detector [2]. We were responsible for their M&O which over the years involved a considerable amount of effort devoted to determining the survivability of the VCSELs (Vertical Cavity Surface Emitting Lasers) used by the pixel and silicon strip (SCT) systems. The VCSELs on the TXs (off-detector transmitters) had to be replaced twice in an unreasonably short time period. The failure was originally attributed to ESD damage however, after the first replacement TXs also failed it was determined that the VCSELs could not survive in the humid environment where the TX boards were located. Since the pixel opto-boards were inaccessible without an extended shut down there was great concern about the reliability of the system. We therefore embarked on two R&D programs at OSU in response to the potential catastrophe.

The first program was the construction of a test system that emulated the ATLAS operating condition of the opto-board VCSEL arrays to systematically study the VCSEL lifetime. The

[2]An opto-board decodes optical bi-phase mark encoded signals from the control room and sends them over copper wires to a pixel module. It also receives signals from a pixel module and converts them to optical signals which are received in the ATLAS control room.

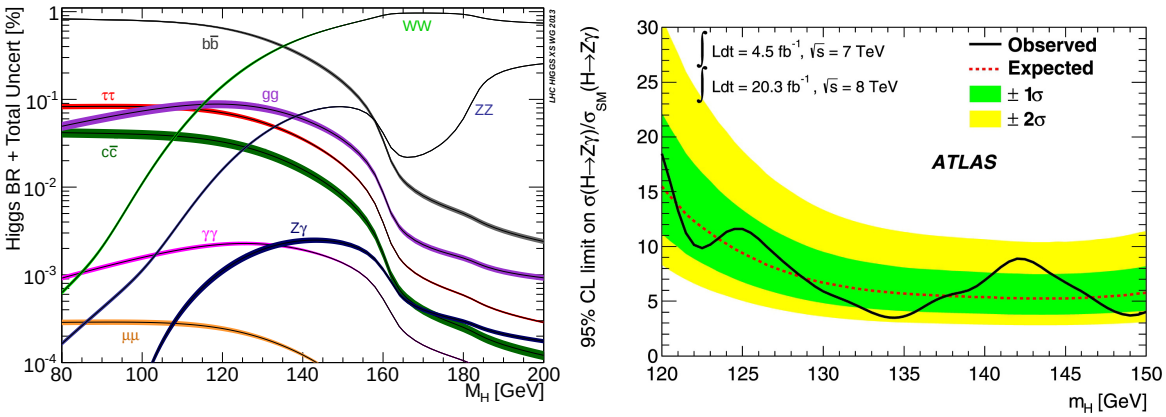

Figure 7: (left) Branching fractions of the SM Higgs boson as a function of mass. (right) Observed 95% CL limits (solid black line) on the production cross section of a SM Higgs boson decaying to $Z\gamma$, as a function of the Higgs boson mass. The median expected 95% CL exclusion limits (dashed red line) are also shown. The green and yellow bands correspond to the 1 and 2σ intervals.

conclusion of the 18-month study was that the installed VCSEL arrays for the pixel detector could survive at least through the year 2021. The second program was to design a new generation of opto-boards in the event that the pixel detector was to be extracted, which as it turned out was the case. The Pixel collaboration decided to extract the pixel detector to allow a safer installation of the insertable barrel layer (IBL), and re-configure the detector's services. The new quarter service panels (nSQP) were relocated to a more serviceable location and hence all of the opto-boards had to be replaced. This required a redesign of the opto-boards for the first three layers and disks of the pixel detector in addition to new opto-boards for the IBL. The extraction of the pixel detector allowed us to perform a postmortem on the opto-boards which revealed that the OSU fabricated opto-boards had a very low failure rate, $\sim$0.1%.

The new opto-boards take advantage of the experience gained from our production and operation of the first generation opto-boards. One major improvement is the re-design of the optical packaging of the VCSEL and PIN arrays. The original opto-packs (from the Taiwan group) had several drawbacks. First, the VCSEL arrays were found to fail under moderate humidity and a suitable replacement had to be found. After measuring the radiation hardness [17] and robustness (e.g. humidity resistance) of several VCSEL arrays we chose an array manufactured by Finisar [18]. We also switched to a more robust PIN array manufactured by ULM [19]. In Fig. 8 we show pictures of the new opto-pack.

Another drawback of the Taiwan opto-packs was the soldering of the micro-leads on an opto-pack to an opto-board. This opto-board was fabricated out of BeO to take advantage of its excellent thermal conductivity. However, this large thermal conductivity made it very difficult to solder a small lead to the BeO substrate. In fact, it has been determined from the postmortem that the major failure mode of an opto-board was due to cold solder joints. To avoid this pitfall the new opto-boards used wire bonds rather than solder [20]. Other improvements included a cost reduction by using polyimide and copper instead of BeO for the PCB, redundant control lines by taking advantage of unused pins on the opto-board's connector, and eliminating the

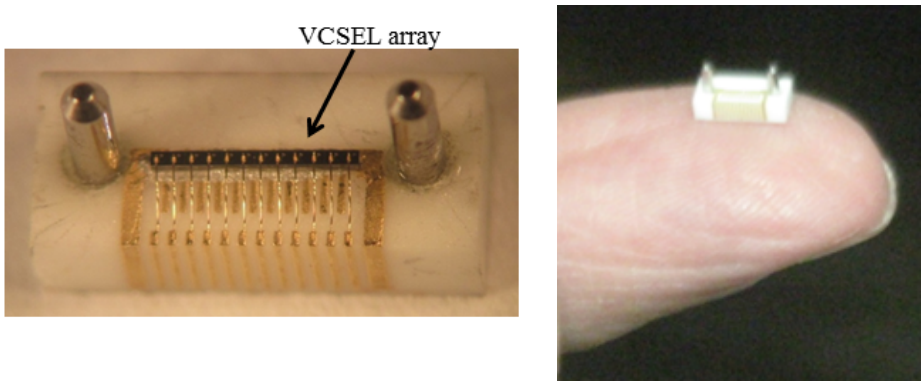

Figure 8: (left) A close up photograph of an opto-pack with a wire bonded VCSEL array. (right) Scale photograph of an opto-pack.

daisy chaining of control signals on the opto-board.

Three varieties of new opto-boards were produced at OSU; IBL, B (originally used by the first layer of the pixel detector), and D (originally used in the disks and second and third layers of the pixel detector). The production of the opto-boards (60 IBL, 55 B, 275 D) was finished in the fall of 2013. The opto-boards are currently installed in ATLAS. In Fig. 9 we show an example of an assembled opto-board. Details of the opto-board production can be found in [21].

1.2.2 Inner Detector Beam Conditions and Beam Loss Monitors

Radiation monitoring plays a crucial role in any experiment which operates a sensitive detector system close to the interaction region. Radiation monitoring also allows for the measurement of the daily and integrated dose which the tracking systems receive and thus allow the prediction of device lifetimes, etc. Finally radiation monitoring devices are excellent choices for luminosity measurement if they have good separation of signal from background either in space or time.

The Beam Conditions Monitor (BCM) detects minimum ionizing particles with good signal-to-noise ratio and a time resolution of ~ 1 ns. Timing is used to distinguish collisions from beam background. For redundancy ATLAS decided to build a second beam loss monitor system, the Beam Loss Monitor (BLM). The choice of diamond sensors for the ATLAS BCM and BLM was motivated by the radiation hardness of diamonds, the high charge carrier velocity and short lifetime leading to very fast and short current signals, the high resistivity leading to very low leakage currents even after extreme radiation, the ability to operate without cooling and the success of previous diamond systems in BaBar [22], Belle and CDF [23] all of which were constructed by OSU personnel. OSU led the design, testing and production of detectors for both the BCM and BLM. Both systems were operational on day one of data taking.

In Fig. 10(a) we show a schematic view of the BCM where the diamond monitors are placed in modules on the forward disks of the pixel detector. A module consists of a box housing two polycrystalline CVD diamonds of 1 cm $\times$ 1 cm area with square contacts 8 mm $\times$ 8 mm mounted back to back. The signals from two sensors are fed in parallel into a very high bandwidth current amplifier. The design aim of a module S/N ratio of $\sim$10:1 in order to detect,

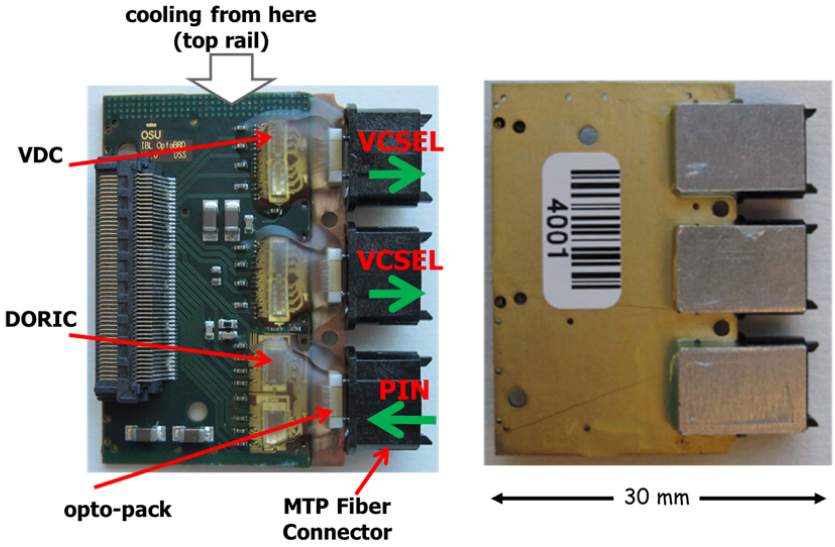

Figure 9: A photograph of the re-designed opto-board showing the VCSEL driver chips (VDCs) that couple to the VCSEL opto-packs and the receiver chips (DORICs) that couple to the PIN opto-pack. Both ASICs were designed by OSU/Siegen for the first generation opto-boards.

with high efficiency, minimum ionizing particles was achieved.

The ATLAS system consists of 10 modules including spares. Figure 10(b) shows a finished module. In Fig. 11(a) we show one half of the final BCM system as it is being installed on the beam pipe. Figure 11 (b) shows the distribution of time differences from hits from the two sides (called A and C) of the BCM. There are three clear peaks: one centered at 0 ns representing true collisions; one centered at +12.5 ns representing Beam 1 background going from side A to side C; and one centered at -12.5 ns representing Beam 2 background going from side C to side A. We observe a single BCM module time resolution of 0.7 ns clearly meeting the design specification without any offline timing corrections.

In addition to being able to determine background from real collisions, the BCM is sensitive enough to abort the LHC beams during potentially dangerous conditions. Figure 12 shows one of the first BCM triggered aborts during an LHC aperture scan. This figure is the postmortem which the BCM sends to the LHC machine group after an abort. The x-axis is the orbit number and the y-axis is the number of BCM hits in an orbit. The postmortem shows the BCM status (number of BCM hits) during the 1,177 orbits prior to the abort and 100 orbits after the abort. This postmortem shows that the LHC beams were hitting something and producing large background during the aperture scan. This is a situation where the beams should be aborted.

The BLM was designed to be the backup or redundant system for the BCM. In Fig. 13(a) we show a schematic view of the BLM where the diamond monitors are placed in the forward

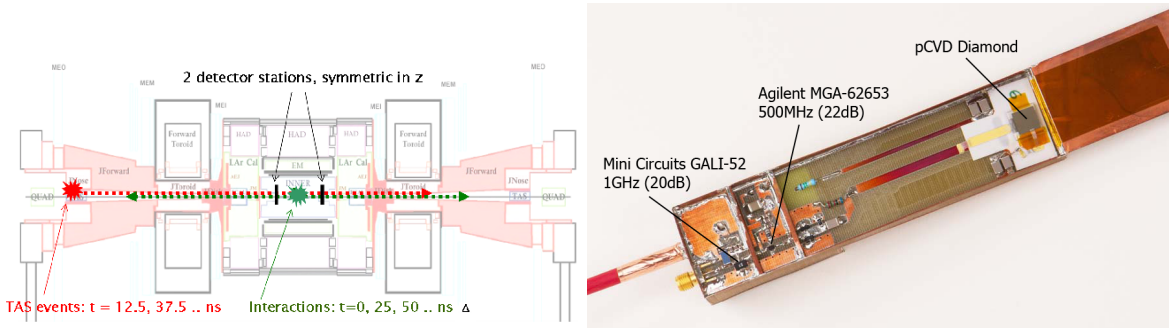

Figure 10: (a) Schematic view of the BCM system. (b) Photograph of the final module used by ATLAS for its BCM system.

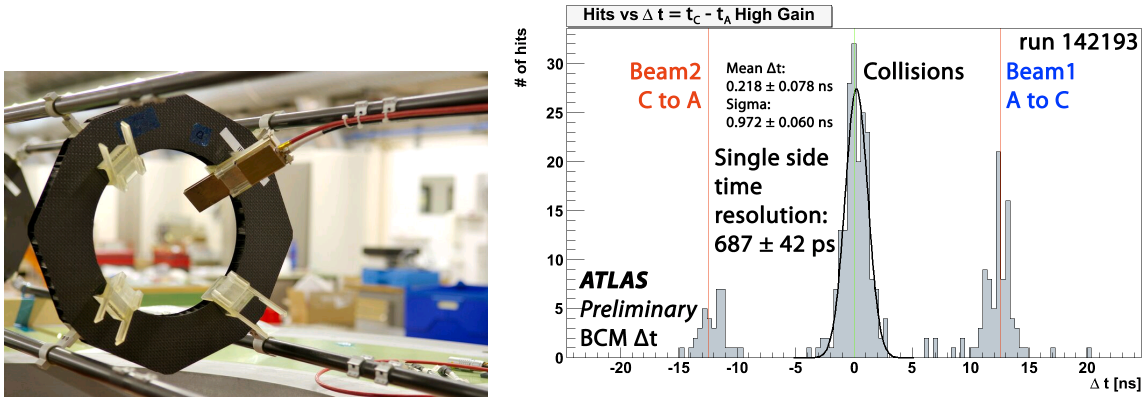

Figure 11: (a) Photograph of one half of the final BCM system during installation on the beam pipe. (b) Time-Of-Flight (TOF) distribution for run 142193 between the two BCM detector stations located at $z = \pm 1.84$ m. Δt values of 12.5 ns represent beam background events from LHC Beam 1 whereas Δt values of -12.5 ns represent LHC Beam 2 background events. Collision events have Δt values of 0 ns. A Gaussian fit of the collision peak yields an individual BCM module time resolution of 0.687 ns.

region just outside of the inner detector. A module consists of a box housing one CVD diamond of 8 mm $\times$ 8 mm area with square contacts 7 mm $\times$ 7 mm. In Fig. 13(b) we show a photograph of a BLM detector and housing. Since April 2010 the BLM has been a part of the LHC abort system.

1.2.3 ATLAS Luminosity Measurement

The BCM was the primary detector used by ATLAS in the 2011 and 2012 luminosity measurements [24]. This function was not originally planned but added due to the speed, robustness and stability of the BCM. Figure 14 shows the output of the BCM luminosity algorithms over the course of a run in both 2010 and 2011. There is remarkable consistency among all algorithms. For the 8 TeV data the uncertainty in luminosity determination is 2.8%.

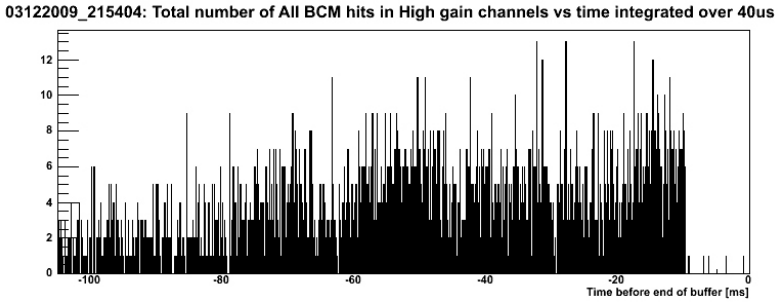

Figure 12: The postmortem generated by a beam dump fired by the BCM during an LHC aperture scan. The x-axis is the orbit number going back 1,177 LHC orbits ($\sim$100 ms) before the beam dump and 100 orbits after the beam dump. The y-axis is the number of BCM hits in an orbit.

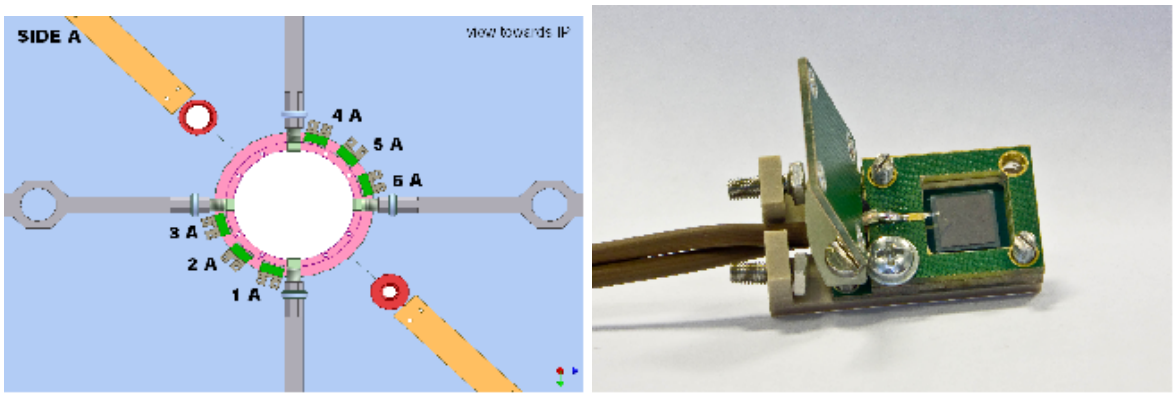

Figure 13: (a) Schematic view of the BLM system. (b) Photograph of a BLM module.

1.2.4 ATLAS Diamond Beam Monitor (DBM)

The ATLAS luminosity is determined to better than 3% primarily by its BCM. Due to its inherent design the BCM will begin to saturate when the instantaneous luminosity reaches $\sim 10^{34}$ cm^{-2}s^{-1} (see Fig. 15). The DBM has been designed to operate without saturation at the highest planned LHC luminosity. The DBM will achieve this by using highly pixelated diamond sensors (25×10^3 pixels/sensor) organized into 8 telescopes with three diamonds per telescope, four telescopes on each side of the interaction region.

For the DBM project the OSU group was responsible for selecting, testing, and qualifying the diamond detectors, working with the University of Toronto on the mechanical design, the thermal simulation of the mechanical design, and the HITBUS chip. The HITBUS chip provides two main functions. The first is collecting trigger information from the HitOr outputs of the DBM telescopes. To perform this function the HITBUS chip has the ability to perform logical operations on the HitOr outputs of each telescope. The second function of the HITBUS chip is to buffer and distribute the control used for configuration of the DBM modules. Fig. 16 shows the DBM PCB with the HITBUS chip mounted (labeled 2227) and installed on the IBL support tube with two DBM telescopes. The DBM was assembled and installed during the fall of 2014 and is awaiting commissioning with beams.

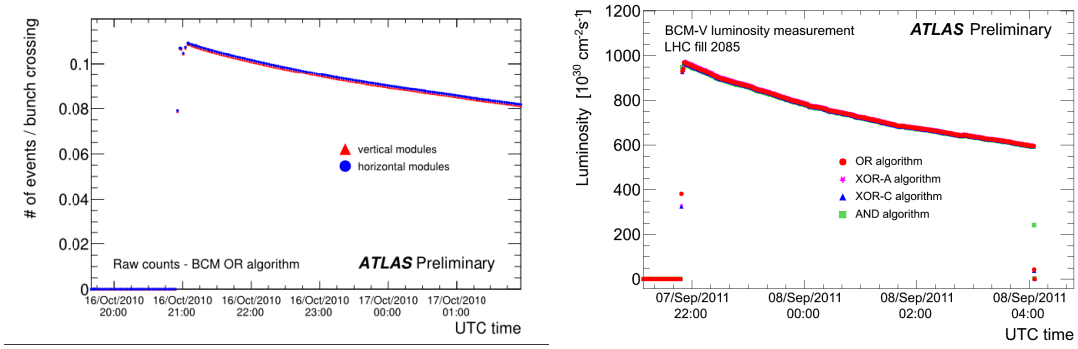

Figure 14: Real-time luminosity measured by the BCM for a run in (a) 2010 and (b) 2011.

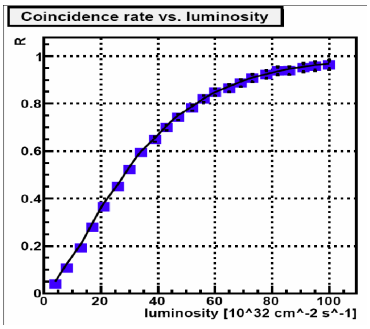

Figure 15: Coincidence rate versus luminosity for the BCM.

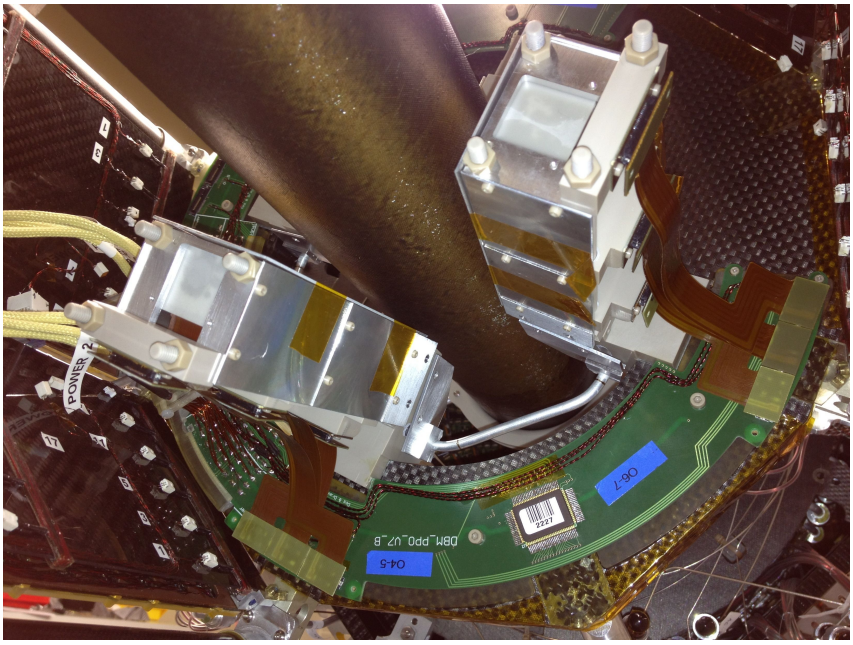

Figure 16: Mounted PP0 board showing the HITBUS chip (labelled 2227) and two DBM telescopes.

1.3 ATLAS Service Work

We have played important roles in the design, construction, and operation of the pixel detector as well as the BCM, BLM, and DBM. Members of our group have held important roles in the operation of the ATLAS detector. For example, H. Merritt and M. Fisher were BCM/BLM Run Coordinators and J. Moss was the Pixel Run Coordinator. D. Pignotti and A. Nagarkar performed detailed measurements of the optical spectra of the VCSELs used in the opto-boards in the effort to better understand their lifetime. Below we list the management and operations tasks in which members of our group have major responsibilities over the last three years.

- H. Merritt was the BCM/BLM Run Coordinator (2011)
- M. Fisher was the Deputy BCM/BLM Run Coordinator (2010)
- J. Moss was the Pixel Run Coordinator (2010)
- K. K. Gan was a member of the US ATLAS Deputy Manager Search Committee (2011-12)
- K. K. Gan was a member of the US ATLAS M&O Manager Search Committee (2010)
- K. K. Gan is a member of the ATLAS Collaboration Board (2007-present)
- K. K. Gan is a member of the ATLAS Pixel Institute Board (2007-present)
- K. K. Gan was Convener of the Joint ATLAS-CMS SLHC Opto-Link Working Group (2009-2010)
- H. Kagan is a member of the ATLAS DBM Institute Board (2011-present)
- H. Kagan is a member of the ATLAS BCM/BLM Institute Board (2007-present).
- H. Kagan is Co-spokesperson of RD42 (2007-present)

1.4 Students awarded a PhD during last grant period

Three of our graduate students received their PhD during the last grant period. Below we list these students.

- Matthew Fisher, "The search for low scale technicolor in the $Z + \gamma$ channel in 7 TeV ATLAS data (2012)."
- Advait Nagarkar, "A measurement of the $W^{\pm}Z$ production cross section and limits on anomalous trilinear gauge couplings in proton-proton collisions at $\sqrt{s} = 7$ TeV using 4.64 fb^{-1} of data collected with the ATLAS detector (2012)."
- Hayes Merritt, "Measurement of the proton-proton to ZZX cross section at a center of mass energy of 8 TeV (2013)."

References

[1] G. Aad *et al.*, "The ATLAS Experiment at the CERN Large Hadron Collider," JINST **3**, S08003 (2008).

[2] K. E. Arms *et al.*, "ATLAS Pixel Opto-Electronics," Nucl. Instr. Meth. A **554**, 458 (2005).

[3] V. Cindro *et al.*, "The ATLAS Beam Conditions Monitor," JINST **3**, P02004 (2008).

[4] M. Mikuz *et al.*, "Diamond Pad Detector Telescope for Beam Conditions and Luminosity Monitoring in ATLAS," Nucl. Instr. and Meth. A **579**, 788 (2007).

[5] H. Kagan, M. Mikuz, W. Trischuk, "ATLAS Diamond Beam Monitor TDR," ATLAS Document ATU_DBM_001, 09/14/2011.

[6] G. Aad *et al.*, "ATLAS Pixel Detector Electronics and Sensors," JINST **3**, P07007 (2008).

[7] G. Aad *et al.*, Phys. Lett. B **716**, 1 (2012).

[8] G. Aad *et al.*, Eur. Phys. J. C **72**, 2173 (2012).

[9] G. Aad *et al.*, Phys. Rev. D **87**, 052004 (2013).

[10] C-H. Chang, Nucl. Phys.B **172**, 425 (1980); R. Baier and R. Ruckl, Phys. Lett. B **102**, 364 (1981); Z. Phys. C 19, 251 (1983); E. L. Berger, D. L. Jones, Phys. Rev. D **23**, 1521 (1981).

[11] H. Fritzsch, Phys. Lett. B **67**, 217 (1977); F. Halzen, Phys. Lett. B **69**, 105 (1977); M. Gluck, J. F. Owens, and E. Reya, Phys. Rev. D **17**, 2324 (1978); V. D. Barger, W. Y. Keung, and R. J. N. Phillips, Phys. Lett. B **91**, 253 (1980); J. F. Amundson, O. J. P. Eboli, E. M. Gregores and F. Halzen, Phys. Lett. B **372**, 127 (1996); J. F. Amundson, O. J. P. Eboli, E. M. Gregores and F. Halzen, Phys. Lett. B **390**, 323 (1997).

[12] A L. Read, J. Phys. G: Nucl. Part. Phys. **28**, 2693 (2002).

[13] Amsler *et al.* (Particle Data Group), Phys. Lett. B **667**, 1 (2008).

[14] K. Lane, "Technihadron Production and Decay in Low Scale Technicolor," Phys. Rev. D **60**, 075007 (1999) and private communications.

[15] G. Azuelos *et al.*, "Low Scale Technicolor at the LHC," arXiv:0802.3715v1[hep-ph].

[16] G. Aad *et al.*, "Search for Higgs boson decays to a photon and a Z boson in pp collisions at $\sqrt{s}$ = 7 and 8 TeV with the ATLAS detector," Phys. Lett. B **732**, 8 (2014).

[17] K.K. Gan *et al.*, "Study of the Radiation-Hardness of VCSEL/PIN," in Proceedings of the 9th International Conference on Large Scale Applications and Radiation Hardness of Semiconductor Detectors, Florence, Italy, 2009, PoS (RD09) 041 (2009); A. Nagarkar *et al.*, "Study of the Radiation-Hardness of VCSEL & PIN Diodes," in Proceedings of the 11th International Conference on Large Scale Applications and Radiation Hardness of Semiconductor Detectors, Florence, Italy, 2011, PoS (RD11) 036 (2011).

[18] The VCSEL array used is V850-2093-001, fabricated by Finisar, Inc.

[19] The PIN array used is ULMPIN-04-TN-U0112U, fabricated by ULM Photonics.

[20] K.K. Gan, "An MT-Style Optical Package for VCSEL and PIN Arrays", Nucl. Instr. and Meth. A **607**, 527 (2009).

[21] R. Kass *et al.*, "The New Radiation-Hard Optical Links for the ATLAS Pixel Detector," to be published in the proceedings of DPF 2013. The presentation can be found at: https://indico.bnl.gov/getFile.py/access?contribId=54&sessionId=17&resId=0& materialId=slides&confId=603.

[22] A.J. Edwards *et al.*, "Radiation Monitoring with CVD Diamonds in BaBar," Nucl. Inst. and Meth. A **552**, 176 (2005).

[23] R. Eusebi *et al.*, "A Diamond-based Beam Condition Monitor for the CDF Experiment," in Proceedings of the 2006 IEEE Nuclear Science Symposium, San Diego, USA, Trans. NSS **2**, 709 (2006).

[24] ATLAS Collaboration, "Luminosity Determination in pp Collisions at $\sqrt{s}$ = 7 TeV using the ATLAS Detector at the LHC," Euro. Phys. J. C **71**,1 (2011).

Task E Final Report

Richard E. Hughes, Brian L. Winer
Department of Physics
The Ohio State University

July 15, 2014

1 Introduction

During this grant cycle Task E had two research concentrations: collider physics and astroparticle physics. Our primary collider physics effort involved the operation and data analysis for the Compact Muon Solenoid (CMS) at CERN (Section 4) and analysis of the final dataset for the Collider Detector at Fermilab (CDF) (Section 3). At the same time we continued our studies with the Fermi Gamma-ray Space Telescope (FGST) (Section 2). This report summarizes our accomplishments of the last three years of the grant. Table 1 lists the personnel that were part of this project during the final three years.

Name	Position	Comments
Richard Hughes	Faculty	co-PI
Brian Winer	Faculty	co-PI
Darren Puigh	Post-doc (CMS)	currently still with group
Homer Wolfe	Post-doc (CDF/CMS)	departed 2012
Zhaoyu Yang	Post-doc (FGST)	departed 2012
Andrea Albert	Graduate Student	Ph.D. May 2013
Sean Flowers	Graduate Student	Ph.D. in progress
Justin Pilot	Graduate Student	Ph.D. August 2011
Geoff Smith	Graduate Student	Ph.D. May 2014
Jonathan Wilson	Graduate Student	Ph.D. December 2011

Table 1: List of personnel during last three years of grant.

2 Fermi Gamma Ray Space Telescope

The Fermi Gamma-ray Space Telescope (FGST) is designed to study high-energy astrophysical phenomena from a variety of sources[1]. The Fermi Large Area Telescope (LAT) detects gamma-rays from 20 MeV to several hundred GeV. Task E interests focused primarily on dark matter searches, though Fermi's overall science program also includes the study of other gamma-ray sources such as pulsars, active galactic nuclei, and gamma-ray bursts. The Task E group contributed to the LAT Collaboration since 2004 and made a number of contributions to the development and testing of the data acquisition system. Since starting science operation five years ago, the group pursued a number of research topics. These analyses included, using gamma-ray bursts to search for evidence of Lorentz Invariance Violation , the search for dark matter in the Milky Way Halo , the measurement of the cosmic-ray proton energy spectrum, and the search for dark matter using gamma-ray spectral lines. During the later part of the grant cycle, OSU was the lead group on the search for dark matter lines. The work on the line analysis has culminated in the submission of an article to *Physics Review D*[2]. We review this analysis below.

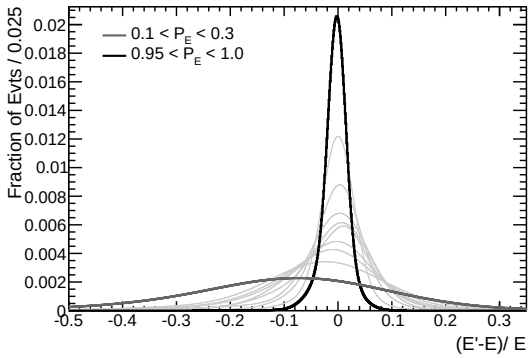

Figure 1: Energy dispersion model for 100 GeV in all 10 P_E bins. The darker lines show the distributions for the smallest and largest values of P_E, while the thinner gray lines show the models for the intermediate P_E bins. (Figure from [2])

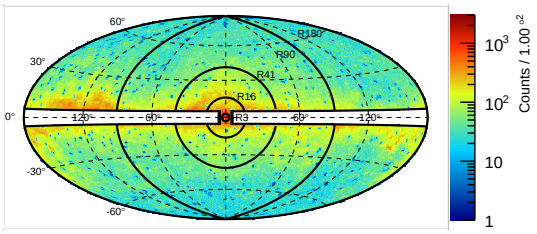

Figure 2: Counts map for the line search dataset binned in $1^\circ \times 1^\circ$ spatial bins. Shown are the outlines of the other ROIs (R3, R16, R41, and R90) used in this search. (Figure from [2])

2.1 Dark Matter Line Search

The existence of a narrow spectral line in the gamma-ray energy spectrum would be strong evidence of dark matter annihilation ($\chi\chi \rightarrow \gamma\gamma$ or γZ) or decay in our galaxy's halo. The analysis formed the core of Dr. Albert's thesis. The search gained significant attention because of claims in the astrophysics community of evidence for a spectral feature near 130 GeV[3, 4, 5, 6, 7]. Through the efforts of the OSU group a number of important optimizations and additions were made to this search. For instance, the line search used a more detailed modeling of a spectral line, which led to increased sensitivity. The search was carried out in a series of regions of interest (ROI) that were optimized for different dark matter profiles in galaxy. In contrast to previous line search analyses, we carried out detailed and comprehensive studies of systematic effects.

Enhanced Line Energy Dispersion Model:

The line analysis developed at OSU used the reprocessed PASS 7 gamma reconstruction software and about four years of LAT data. One of the major improvements to the analysis was the adoption of a new dispersion model for a gamma-ray line. Our new model for the LAT energy dispersion incorporates both the energy and a variable that quantifies the quality of the energy measurement called CTBBestEnergyProb (P_E). Cleaner and/or better reconstructed events have a P_E closer to 1 while events with a poorer reconstruction have a value closer to 0. Consequently, the energy dispersion is much sharper for high P_E events and becomes wider with a bias towards under-measuring the energy for low P_E events. Figure 1 shows the energy dispersion for monte carlo events with different ranges of P_E. The two darkest lines show the extremes. Using this extra piece of information significantly improved the modeling, especially in the tails of the distribution. Furthermore, by using this additional information, we increased by ∼15% our sensitivity for significantly detecting a line. We also improved the expected limits in a null-DM scenario by ∼10%.

Optimized Regions of Interest:

Previous Fermi-LAT dark matter line searches included data from the full sky, except for a thin slice corresponding to the galactic plane away from the galactic center. While N-body simulations expect dark matter to be concentrated in the galactic center, there is substantial uncertainty as to the amount of concentration or cuspiness. For the our analysis, we performed an optimization of the region of interest (ROI) for several different proposed dark matter profiles. Each region is centered on the galactic center and has a different angular radius from the center. We continue to mask out a region covering the galactic plane (away from the center). The ROIs considered in this analysis are shown in Figure 2. There are five separate regions: R3, optimized for a contracted NFW profile[8]; R16, optimized for an Einasto profile[9]; R41, optimized for an NFW profile[8]; R90, optimized for an Isothermal profile[10]; and R180, ("full" sky) used as a comparison to the previous published result and appropriate for dark matter decays, rather than annihilations.

Table 2: Summary of systematic effects. (Adapted from [2])

Systematic	ROI/Energy Constraint	Effect	
Effective area scale		$\delta\mathscr{E}/\mathscr{E} =$	± 0.1
Averaging exposure over ROI	(R3)	$\lvert\delta\mathscr{E}/\mathscr{E}\rvert <$	0.01
	(R180, $E_\gamma = 300$ GeV)	$\delta\mathscr{E}/\mathscr{E} =$	± 0.13
E_γ grid spacing		$\delta n_{\rm sig}/n_{\rm sig} =$	$^{+0.0}_{-0.1}$
Energy resolution		$\delta n_{\rm sig}/n_{\rm sig} =$	± 0.07
Broadening from Z width	($E_\gamma = 68$ GeV)	$\delta n_{\rm sig}/n_{\rm sig} =$	-0.07
P_E distribution variation		$\delta n_{\rm sig}/n_{\rm sig} =$	± 0.01
Energy dispersion model θ-variation		$\delta n_{\rm sig}/n_{\rm sig} =$	± 0.02
CR contamination	(R3)	$\lvert\delta f\rvert <$	0.005
	(R180)	$\delta f =$	± 0.014
Point-source contamination		$\lvert\delta f\rvert <$	0.005
Effective area variations	($E_\gamma = 5$ GeV)	$\delta f =$	± 0.005
	($E_\gamma > 100$ GeV)	$\delta f =$	± 0.025
Astrophysical background modeling	(R180, $E_\gamma = 30$ GeV)	$\delta f =$	± 0.005
	(R180, $E_\gamma > 100$ GeV)	$\delta f =$	± 0.011
	(R3)	$\delta f =$	± 0.019

Studies of Systematic Uncertainties:

As the data sample size becomes large it is more and more important to consider a wide variety of systematic errors that could potentially introduce a false signal (or mask a true signal) and impact our limits. Previous analyses treated a small set of systematic errors in limited detail. In our analysis, we considered a wide variety of uncertainties that can impact the result in a variety of ways. We classified those uncertainties into three categories: (1)Uncertainties that enter in the conversion between the fit number of signal counts, $n_{\rm sig}$, and the inferred fluxes. These uncertainties induced a corresponding uncertainty in the estimated model fluxes and upper limits on those fluxes, but do not affect fit significance. We quantified these in terms of the relative uncertainty of the exposure: $\delta\mathscr{E}/\mathscr{E}$. (2) Uncertainties that scaled the fit estimates of the number of signal counts (i.e., affect fit significance and upper limits) but would not otherwise induce or mask a signal. These primarily consist of errors in signal model parameterization. We quantified these in terms of the relative uncertainty of the number of signal counts: $\delta n_{\rm sig}/n_{\rm sig}$. (3)Uncertainties that could mask a true signal, or induce a false signal. We quantify these in terms of the induced fractional signal, f. Table 2 summarizes the findings of our systematic studies.

Putative Gamma-ray Line near 130 GeV

In 2012, a number of independent papers appeared in the literature reporting the detection of a line-like feature in the Fermi-LAT data localized around the galactic center[3, 4, 5, 6, 7]. We have performed a careful analysis of this region using our new analysis techniques and considering several important control regions. Our fit in ROI R3 is shown in Figure 3. In our analysis of this feature, we discovered several important features, which are reported in our publication. First, when performing the fit on the reprocessed data the best fit line shifts from ∼130 GeV to 133 GeV, as would be expected from the updated calibrations. Second, when we use our new energy dispersion model, the statistical significance of the line is reduced. This was primarily due to the feature in the data being too narrow compared to our expected resolution, as can be seen in Figure 3. In fact, we determined that our energy resolution would need to be about a factor of three times better to observe a feature so narrow. This is far beyond the expected uncertainty on the Fermi-LAT energy resolution. Finally, investigations of a control sample consisting of photons from the earth's limb, which are created by cosmic ray interactions with the earth's atmosphere, exhibited a line-like feature also around 130 GeV. This control sample should be free of any dark matter signal. Although the feature in the earth's limb is not of sufficient size to fully explain the line seen in the galactic center, it does support the idea that this was due to a systematic reconstruction effect.

95% Confidence Level Limits

Our line analysis found no globally significant gamma-ray lines in any of the ROIs. We proceeded to set limits on dark matter annihilation in each ROI for the corresponding dark matter profile. The limits for R16,

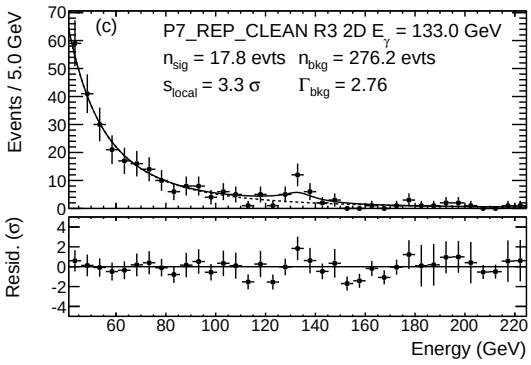

Figure 3: Fits for a line near 130 GeV in R3: using the 2D energy dispersion model. (Figure from [2])

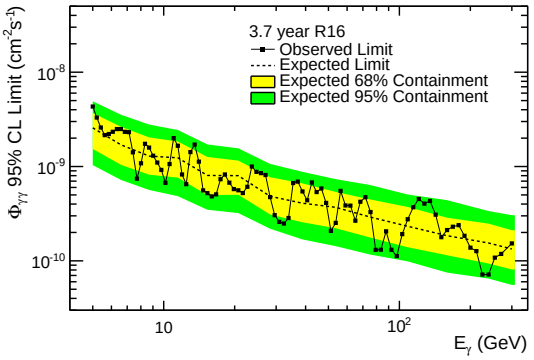

Figure 4: 95% CL $\Phi_{\gamma\gamma}$ in the R16 ROI (black points).(Figure from [2])

optimized for the Einasto profile, are shown in Figure 4. As can be seen in the figure, the observed limits are consistent with our *a priori* predictions, shown as the yellow and green bands.

3 Collider Detector at Fermilab Experiment

The Ohio State group has contributed significant personpower and leadership to the CDF Experiment in detector development, data taking operations, and physics results.

As of September, 2011, the Fermilab Tevatron ceased collider operations. This ended an incredibly successful run: 26 years since initial collisions began in 1985, and just under 11 years since the beginning of Run II. The performance of the both the Tevatron and the CDF detector - particularly over the Run II time-frame - was outstanding. The total Run II acquired luminosity was just under 10 fb^{-1}. Both our group and the larger collaboration put enormous effort into turning this windfall of data into physics results for publication and presentation at conferences. At the beginning of Run II, the Higgs Boson was the one remaining discovery expected from the Standard Model, and establishing its existence or bounding its mass was a primary goal of the Tevatron collider physics program. This is where we have placed the majority of the group's resources over the years fromn 2006-2013

3.1 The Search for the Standard Model Higgs Boson at CDF

The search for the standard model Higgs boson at CDF was the product of ten separate physics analyses performed by approximately 50 researchers. The Ohio State group contributed significantly to four of the six most sensitive subchannels. A wealth of publications resulted from these searches: 12 publications [11] [12] [13] [14] [15] [16] [17] [18] [19] [20] [21] [22] in 2012, of which 7 were in Physical Review Letters; and 6 publications [23][24][25][26][27][28] in 2013, of which 2 were in Physical Review Letters.

The standard model Higgs boson was predicted to be present in CDF data, but distributed over many distinct final states. While a light ($m_H < 135$) Higgs boson is predicted to decay predominantly to pairs of b quarks, QCD multijet production of b jets overwhelms the predicted signal. The SM Higgs boson is also predicted to be produced in association with other particles like pairs of top quarks (ttH), W bosons (WH), and Z bosons (ZH). Selecting events with leptonic decays of W and Z bosons serves to suppress backgrounds, making associated production searches the most sensitive at the Tevatron to a light SM Higgs boson. The top five searches, at the Tevatron, in order of their sensitivity to a light SM Higgs boson, are given in Table 3.1. The OSU group directly contributed to all of these analyses, with 5 graduate students performing their thesis analyses in the Higgs group. Directly contributing to the results below are former OSU graduate students Dr. Justin Pilot (now a postdoctoral researcher for UC Davis on CMS), and Dr. Jon Wilson (who went on to become a postdoctoral researcher for UM on CDF and Nova). In addition, Ohio State post-dcotoral researched Dr. Homer Wolfe served the CDF Collaboration as the Deputy Convener of the Higgs Discovery Group, and the WH Analysis Group Co-Convener.

Sensitivity Rank	Channel	Expected/Observed Limit×SM (at $M_H = 120\ GeV/c^2$)	OSU Contribution
1	$WH \to l\nu b\bar{b}$	2.3/4.3	Analysis execution
2	$ZH \to l^+l^- b\bar{b}$	3.1/5.7	Analysis execution New analysis technique
3,4	$ZH, WH \to$MET$b\bar{b}$	3.1/3.9	New analysis technique
5	$t\bar{t}H \to l\nu$+Jets	11.6/19.0	Analysis initiation Analysis execution

Table 3: The five most sensitive subchannels in the CDF standard model Higgs search, ranked by sensitivity contribution to the combined result for a low-mass standard model Higgs boson.

3.2 Analysis Contributions

The OSU group has had a proud history of improving the sensitivity of Higgs searches beyond what is expected from increased data set size. In time period from 2010-2013, the analysis framework developed and managed by Homer Wolfe was adopted by the $l\nu bb$ group and the $llbb$ group, and was used to develop the ttH analysis.. This framework combined the previous analysis improvements of several physics analyses at CDF, and allowed the efficient deployment of a newly developed b-jet identification algorithm. In the $llbb$ analysis, Justin Pilot developed multivariate lepton identification which improved signal acceptance by more than 10%. Homer Wolfe developed a method of modeling inclusive online event selection that further improved the analysis sensitivity by approximately 20%. This method was then propagated to the MET$b\bar{b}$ channel with similarly dramatic results. The OSU group also initiated the ttH analysis, which had never before been included in the CDF combined search, and had sensitivity which surpassed that of searches in several other channels.

3.3 Combined Higgs Boson Search Results

Three combined searches for the SM Higgs boson were performed at the Tevatron: CDF, D0, and CDF+D0. The expected exclusion sensitivity to a low-mass Higgs boson by the CDF combination is roughly 20% more sensitive than that of the D0 combination. The Tevatron combined Higgs search has an expected exclusion sensitivity of 1.1 times the SM rate or better for a low-mass Higgs, as is shown in Fig. 5. While the sensitivity of Higgs searches at the LHC are dominated by searches where the Higgs boson decays into pairs of photons, W bosons, or Z bosons, sensitivity to the SM Higgs boson at the Tevatron is driven by decays to pairs of b quarks. The expected exclusion sensitivity of $H \to b\bar{b}$ for the Tevatron combination is currently stronger than that for the same analysis at CMS and ATLAS. In Fig 6, the measured cross section for a SM Higgs boson under several mass hypotheses is shown. At ≈ 125 GeV/c^2, an excess of ≈ 3 standard deviations over the background is seen, and the measured cross section times branching fraction is compatible with the standard model prediction to within 1.5 standard deviations.

4 Compact Muon Solenoid Experiment

4.1 Search for $t\bar{t}H \to \ell^{\pm}\nu q\bar{q}b\bar{b}$H

After the discovery of a new boson in 2012, the emphasis shifted towards measurements of its couplings. Our group led the effort in establishing a new group to measure the Higgs-top Yukawa coupling, through the search for and eventual observation of $t\bar{t}H \to \ell^{\pm}\nu q\bar{q}b\bar{b}$H production. The distinctive decay products of this production mechanism reduce the otherwise large QCD background of the $H \to b\bar{b}$ decay. The $t\bar{t}H \to \ell^{\pm}\nu q\bar{q}b\bar{b}$H mechanism is the only production mode directly sensitive to Higgs-to-top coupling. Furthermore, searching for $t\bar{t}H \to \ell^{\pm}\nu q\bar{q}b\bar{b}$H can also be used to probe models beyond the Standard Model that predict increased rates of $t\bar{t}H \to \ell^{\pm}\nu q\bar{q}b\bar{b}$H production without changing Higgs branching ratios.

The analysis aimed at $H \to b\bar{b}$ was divided into two main subsets: one in which the top quarks produce a single lepton from the leptonic decay of one of the W bosons (lepton+jets), and one in which both W bosons from the top quark pair decays to leptons (dilepton). After requiring an intitial event selection involving kinematics, object identification and quality cuts, we categorized each of the events based on the number of

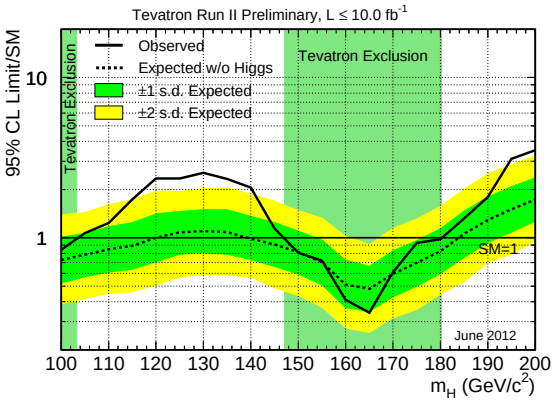

Figure 5: Combined CDF and D0 upper confidence limits on the cross section times branching fraction for a SM Higgs boson, shown as a ratio to the standard model prediction. The search is performed for mass hypotheses $m_H = 100$ to 200 GeV. The most significant departure from the expected exclusion is in the range 120 – 135 GeV/c^2.

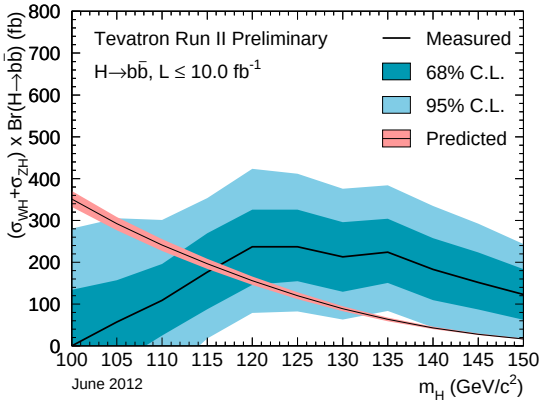

Figure 6: Combined CDF and D0 maximum posterior liklihood distributions for the cross section times branching fraction for $H \to b\bar{b}$. The SM theory prediction for each mass hypothesis is shown overlayed.

jets they contain, as well as the number of jets identified as originating from bottom quarks ("b-tagged" jets). Figure 7 (left) shows the number of events in the different categories for data, background expectation, and signal. Through this categorization, our sensitivity is increased in events that are more signal-like, while the more background-like events serve as control regions.

Although we are able to achieve significant background rejection in our signal-like categories , there was no simple discriminating variable we could use to isolate our signal. To further improve signal sensitivity, we trained boosted decision trees (BDT) to distinguish between signal and background in each of the categories. To train these networks, we used event kinematics, shape, and b-tagging information. The BDT responses were fed into a statistics program, which performs a simultaneous fit for signal and background fractions across all of the different categories.

For our studies we used approximately 19 fb^{-1} of pp collision data collected at a center-of-mass energy of 8 TeV. Figure 7 (right) shows our observed and expected limits as a function of $m_H$for all search channels combined. Results can be found in our paper that has been accepted by the journal JHEP [29] and a publication that is in preparation.

4.1.1 L1 Trigger Upgrades

In 2013, the LHC accelerator complex and the experiments entered *Long Shutdown 1* (LS1). The shutdown will allow for necessary improvements to the accelerator, which will allow it to reach its design center of mass energy of 14 TeV and an increase in the instantaneous luminosity ($\sim 2 \times 10^{34}\ cm^{-2}\ s^{-1}$). One of the proposed upgrades to CMS will be an improved Level-1 Trigger System. One of the biggest challenges will be triggering effectively at these high luminosities since there will be 50-100 overlapping collisions, or "pile-up" (PU), per beam crossing. In 2012 and 2013, we contributed to the preparation of the Level-1 Trigger Upgrade Technical Design Report (TDR). This report was submitted to the LHCC in May 2013 [30]. This design report evaluated the performance of the current L1 trigger system in the post-LS1 environment and define the scope of upgrades to the Level-1 system that are necessary to cope with challenging beam conditions.

Winer was co-leader of the *Level-1 Trigger Upgrade Performance Task Force*. The Task Force was charged with projecting the performance of the current Level-1 trigger system and the performance of the improved trigger algorithms made possible by the proposed hardware upgrades. Our group developed code to measure and extrapolate trigger rates to higher luminosity. These extrapolations used special high pileup fills from 2012 LHC running. Although the instantaneous luminosity in these fills was low, we extrapolated to higher luminosity assuming a full complement of LHC bunches at 50 ns spacing.

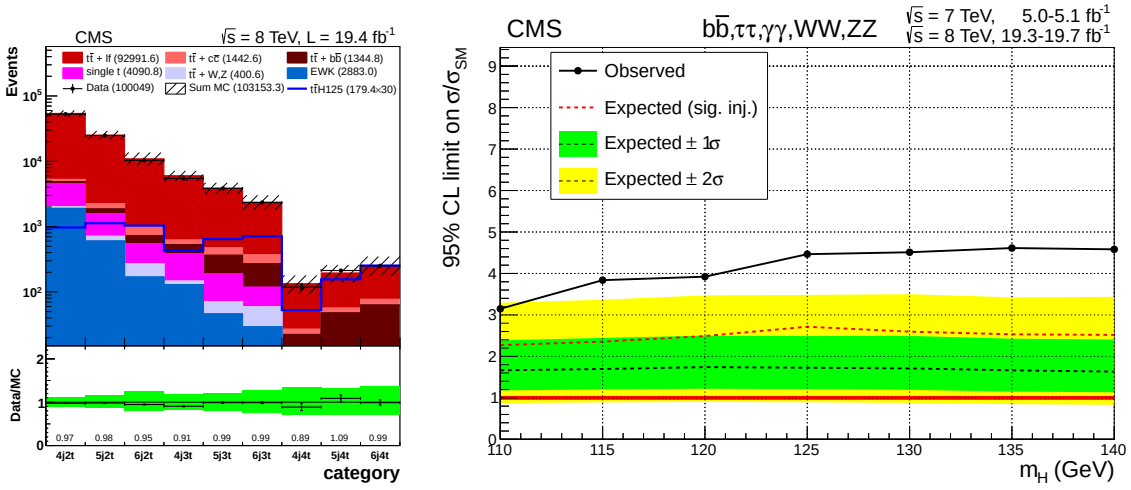

Figure 7: Left: Illustrating the number of events in the different categories based on the number of jets and b-tagged jets for data (black points), background (stacked histograms), and $t\bar{t}H \rightarrow \ell^{\pm}\nu q\bar{q}b\bar{b}$H signal (blue line). The background is normalized to the SM expectation; the uncertainty band (shown as a hatched band in the stack plot and a green band in the ratio plot) includes statistical and systematic uncertainties that affect both the rate and shape of the background distributions. The $t\bar{t}H \rightarrow \ell^{\pm}\nu q\bar{q}b\bar{b}$H signal (m_H= 125 GeV/c^2) is normalized to 30 × SM expectation. Right: The expected and observed limit for the ttH analysis with CMS data and using all search channels.

Next, we estimated the Level-1 thresholds required to maintain the overall Level-1 trigger rate below 100 kHz, the limit for low deadtime operation. For the purpose of these studies we considered two benchmark operational points, $\sqrt{s} = 14$ TeV with $L = 1.1 \times 10^{34}$ cm^{-2}s^{-1} and 50 ns bunch spacing, and $\sqrt{s} = 14$ TeV with $L = 2.2 \times 10^{34}$ cm^{-2}s^{-1} and 25 ns bunch spacing. In both of these cases, the average pile-up is expected to be fifty. Defining trigger thresholds requires the development of a *L1 Menu*, the collection of trigger algorithms that will be run simulataneous. Since the total Level-1 trigger rate is not the simple sum of individual trigger rates, due to single events possibly firing multiple algorithms, the full L1 Menu must be considered. All the trigger algorithm must be considered simultaneously for each data or monte carlo event. The total Level-1 rate was then defined as the rate of events passing any one or more trigger algorithms. We developed code that performed the rate evaluations for L1 Menus and properly accounted for the correlations between triggers. The procedure we developed also automatically determined where indivdual trigger thresholds needed to be set such that the total Level-1 rate remained below the 100 kHz value. This procedure was used to demonstrate that the Level-1 thresholds would need to be set quite high using the Run I trigger system. For example, at $L = 2.2 \times 10^{34}$ cm^{-2}s^{-1}, the Single e/γ trigger would need the $E_T$threshold set at 67 GeV. Through this work it was shown that keeping the current Level-1 trigger system would compromise the potential future physics reach of CMS.

The entire procedure of evaluating trigger rates and L1 Menus was repeated using emulations of the upgraded system. The proposed upgrade was a much more flexible trigger system that allows more sophosticated algorithms. Some of these improvements include, better muon $p_T$assignment, more efficient tau identification, and jet reconstruction with pile-up subtraction. These improvements will help control trigger rates and allow us to operate at lower thresholds than would be possible with the Run I system.

The Level-1 Trigger studies developed for the TDR were extended to running of the LHC after *Long Shutdown 2*. We performed a series of studies to investigate the performance of the upgraded trigger when further improvements of the luminosity occur. These studies considered beam conditions of up to $L = 5.6 \times 10^{34}$ cm^{-2}s^{-1} and pile-up of 140. In contrast to the TDR, which demanded the total Level-1 bandwidth remain below 100 kHz, these studies considered a variety of possible bandwidths between 100 kHz and 1 MHz. One of the most important results of the this study centered on the use of Level-1 tracks in the trigger system after Long Shutdown 2. Our studies showed that having a system that used tracks in the Level-1 trigger decision had the potential to lower the overall trigger rate by a factor of approximately five. This coupled with extending the Level-1 total bandwidth to at least 500 kHz would allow the trigger system to

maintain thresholds that were similar to those proposed in Run 2 (post Long Shutdown 1) and therefore maintain the current physics reach of the CMS detector. These studies are being included in a Technical Proposal, which is currently being drafted.

References

[1] Fermi-LAT Collaboration, W. B. Atwood *et al.*, The Large Area Telescope on the Fermi Gamma-Ray Space Telescope Mission, Astrophys.J. **697**, 1071 (2009), arXiv:0902.1089.

[2] Fermi-LAT Collaboration, M. Ackermann *et al.*, Search for Gamma-ray Spectral Lines with Fermi Large Area Telescope and Dark Matter Implications, Submitted to Phys. Rev D. May 24 (2013), arXiv:1305.5597.

[3] C. Weniger, A Tentative Gamma-Ray Line from Dark Matter Annihilation at the Fermi Large Area Telescope, JCAP **1208**, 007 (2012), arXiv:1204.2797.

[4] E. Tempel, A. Hektor, and M. Raidal, Fermi 130 GeV gamma-ray excess and dark matter annihilation in sub-haloes and in the Galactic centre, JCAP **1209**, 032 (2012), arXiv:1205.1045.

[5] M. Su and D. P. Finkbeiner, Strong Evidence for Gamma-ray Line Emission from the Inner Galaxy, (2012), arXiv:1206.1616.

[6] A. Hektor, M. Raidal, and E. Tempel, An evidence for indirect detection of dark matter from galaxy clusters in Fermi-LAT data, (2012), arXiv:1207.4466.

[7] M. Su and D. P. Finkbeiner, Double Gamma-ray Lines from Unassociated Fermi-LAT Sources, (2012), arXiv:1207.7060.

[8] J. F. Navarro, C. S. Frenk, and S. D. M. White, The Structure of Cold Dark Matter Halos, Astrophys.J. **462**, 563 (1996), arXiv:astro-ph/9508025.

[9] J. F. Navarro *et al.*, The diversity and similarity of simulated cold dark matter haloes, MNRAS **402**, 21 (2010), arXiv:0810.1522.

[10] J. N. Bahcall and R. M. Soneira, The universe at faint magnitudes. I - Models for the galaxy and the predicted star counts, Astrophys.J.Suppl. **44**, 73 (1980).

[11] CDF Collaboration, T. Aaltonen *et al.*, Search for the standard model Higgs boson produced in association with top quarks using the full CDF data set, Phys.Rev.Lett. **109**, 181802 (2012), 1208.2662.

[12] CDF Collaboration, D0 Collaboration, T. Aaltonen *et al.*, Evidence for a particle produced in association with weak bosons and decaying to a bottom-antibottom quark pair in Higgs boson searches at the Tevatron, Phys.Rev.Lett. **109**, 071804 (2012), 1207.6436.

[13] CDF Collaboration, T. Aaltonen *et al.*, Search for a Higgs boson in the diphoton final state using the full CDF data set from proton-antiproton collisions at $\sqrt{s} = 1.96$ TeV, Phys.Lett. **B717**, 173 (2012), 1207.6386.

[14] CDF Collaboration, T. Aaltonen *et al.*, Novel inclusive search for the Higgs boson in the four-lepton final state at CDF, Phys.Rev. **D86**, 072012 (2012), 1207.5016.

[15] CDF Collaboration, D0 Collaboration, T. Aaltonen *et al.*, Search for Neutral Higgs Bosons in Events with Multiple Bottom Quarks at the Tevatron, Phys.Rev. **D86**, 091101 (2012), 1207.2757.

[16] CDF Collaboration, T. Aaltonen *et al.*, Search for the standard model Higgs boson decaying to a $b\bar{b}$ pair in events with no charged leptons and large missing transverse energy using the full CDF data set, Phys.Rev.Lett. **109**, 111805 (2012), 1207.1711.

[17] CDF Collaboration, T. Aaltonen *et al.*, Combined search for the standard model Higgs boson decaying to a bb pair using the full CDF data set, Phys.Rev.Lett. **109**, 111802 (2012), 1207.1707.

[18] CDF Collaboration, T. Aaltonen *et al.*, Search for the standard model Higgs boson decaying to a bb pair in events with two oppositely-charged leptons using the full CDF data set, Phys.Rev.Lett. **109**, 111803 (2012), 1207.1704.

[19] CDF Collaboration, T. Aaltonen *et al.*, Search for the standard model Higgs boson decaying to a bb pair in events with one charged lepton and large missing transverse energy using the full CDF data set, Phys.Rev.Lett. **109**, 111804 (2012), 1207.1703.

[20] CDF Collaboration, T. Aaltonen *et al.*, Search for the standard model Higgs boson produced in association with a $W^{\pm}$ boson with 7.5 fb^{-1} integrated luminosity at CDF, Phys.Rev. **D86**, 032011 (2012), 1206.5063.

[21] CDF Collaboration, T. Aaltonen *et al.*, Search for the standard model Higgs boson produced in association with a Z Boson in 7.9 fb(-1) of p anti-p collisions at $\sqrt{s} = 1.96$ TeV, Phys.Lett. **B715**, 98 (2012), 1203.5815.

[22] CDF Collaboration, T. Aaltonen *et al.*, Search for a low mass Standard Model Higgs boson in the $\tau - \tau$ decay channel in $p\bar{p}$ collisions at $\sqrt{s} = 1.96$ TeV, Phys.Rev.Lett. **108**, 181804 (2012), 1201.4880.

[23] CDF Collaboration, T. Aaltonen *et al.*, Searches for the Higgs boson decaying to $W^+W^- \to \ell^+\nu\ell^-\bar{\nu}$ with the CDF II detector, Phys.Rev. **D88**, 052012 (2013), 1306.0023.

[24] CDF Collaboration, D0 Collaboration, T. Aaltonen *et al.*, Higgs Boson Studies at the Tevatron, Phys.Rev. **D88**, 052014 (2013), 1303.6346.

[25] CDF Collaboration, T. Aaltonen *et al.*, Combination of Searches for the Higgs Boson Using the Full CDF Data Set, Phys.Rev. **D88**, 052013 (2013), 1301.6668.

[26] CDF Collaboration, T. Aaltonen *et al.*, Updated search for the standard model Higgs boson in events with jets and missing transverse energy using the full CDF data set, Phys.Rev. **D87**, 052008 (2013), 1301.4440.

[27] CDF Collaboration, T. Aaltonen *et al.*, Search for a two-Higgs-boson doublet using a simplified model in $p\bar{p}$ collisions at $\sqrt{s} = 1.96$ TeV, Phys.Rev.Lett. **110**, 121801 (2013), 1212.3837.

[28] CDF Collaboration, T. Aaltonen *et al.*, Search for the Higgs boson in the all-hadronic final state using the full CDF data set, JHEP **1302**, 004 (2013), 1208.6445.

[29] CMS Collaboration, S. Chatrchyan *et al.*, Search for the standard model Higgs boson produced in association with a top-quark pair in pp collisions at the LHC, (2013), 1303.0763.

[30] CMS Collaboration, CMS Technical Design Report for the Level-1 Trigger Upgrade, (2013).

Final Report for the period 12/1/2010-4/30/2014

TASK R

DE-FG02-91ER40690

K. Honscheid, R. Kass

Department of Physics
The Ohio State University
191 West Woodruff Avenue
Columbus, Ohio 43210

July 2014

Task R Overview

Historically, The Ohio State University high energy physics group established a very strong presence on the BaBar experiment with major responsibilities in areas of hardware and software. However, over the period of this grant the PIs transitioned to the energy frontier (Kass) and the cosmic frontier (Honscheid) and therefore the activities on this grant were extremely limited.

Below we list our major accomplishments on BaBar over the lifetime of the grant.

- Data taking with BaBar and the successful operation of the BaBar Limited Streamer Tube (LST) muon/K_L detection system and CVD diamond based radiation monitor for the silicon vertex tracker.
- BaBar analysis projects in the area of B-meson, τ, and charm physics.
- Operation of a Monte Carlo farm.
- Service work for the BaBar experiment including serving on paper review committees and reviewing on-going physics analysis projects.
- Editing the chapter on hadronic B decays to charm for the "Physics of B-Factories" book [1].

1 The Ohio State University Task R Program

The faculty of this Task along with Profs. Gan and Kagan joined BaBar in May 2002. Our move from CLEO to BaBar reflected our belief that the study of e^+e^- collisions in the $\Upsilon(4S)$ energy region at high luminosity offered an extremely rich and exciting physics program. We were major contributors to several key areas including the operation of a Monte Carlo (MC) production farm at OSU; the design, construction, installation, and operation of the Instrumented Flux Return (IFR) muon/K_L detector based on Limited Streamer Tube technology[2]; the design, construction and installation of new radiation monitors for BaBar's silicon vertex tracker (SVT) based on CVD diamond detectors [3]; software development for tracking, prompt reconstruction and production; and physics analysis in the areas of tau, charm and bottom decays.

Over the past years this group's activities on BaBar were phased out as we transitioned to other projects such as ATLAS at CERN's Large Hadron Collider (LHC) and non-accelerator physics projects such as BOSS, DES and LSST. Consistent with our ramp up on ATLAS and non-accelerator physics our BaBar group's personnel has contracted to the point where only PIs Honscheid and Kass were supported on this Task over the last grant period.

1.0.1 Recent BaBar management and service tasks

Members of our group played an important role in BaBar management and data processing. Below we list areas where members of our group recently had major responsibilities.

- K. Honscheid was a member of the Publications Board.
- K. Honscheid was a member of the BaBar Beyond 2008 Task Force.
- R. Kass was a member of the Speaker Bureau.
- R. Kass was a member of the Publications Board.
- R. Kass was a member of the BaBar Executive Committee.
- R. Kass was a member of the Spokesperson Search Committee (2008).

1.0.2 BaBar Physics Analysis

The OSU group has already published results in the areas of $\Upsilon(3S)$, τ, charm, and B physics. In FY12 we published one analysis on charm physics which we will briefly describe.

1.0.2.1 Measurement of $\mathcal{B}(D^0 \to \pi^0\pi^0$ and search for $D^0 \to \gamma\gamma$) (Honscheid, Kass, Morris) In the standard model flavor changing neutral currents (FCNC) are forbidden at tree level and for charm meson decays because of the rather light down-quark sector even loop level diagrams are strongly suppressed via the GIM mechanism [4]. However, additional amplitudes in many models for physics beyond the standard model including supersymmetric scenarios with R-parity violation could result in significantly larger branching fractions for $c \to u\gamma$ transitions [5]. Using a data sample corresponding to 470 fb^{-1} collected with the BaBar detector we searched for rare doubly radiative decays of D mesons, $D^0 \to \gamma\gamma$ and in the same analysis provided an improved measurement of $\mathcal{B}(D^0 \to \pi^0\pi^0)$. In order to avoid uncertainties in the production cross section for charm mesons we extract the signal yield in both studies relative to the well measured decay $D^0 \to K_s\pi^0$. Combinatoric background was reduced by requiring our D meson candidates to originate from a D^{*+} decay. A lower threshold on the D^{*+} momentum suppresses most backgrounds from B meson decays. An extended unbinned maximum likelihood fit was used to extract the signal yield from the invariant mass distribution of accepted D^0 meson candidates. In Fig. 1 (left) we show the invariant mass distribution of $D^0 \to \pi^0\pi^0$ candidates. We find $25,964 \pm 305$ signal events in the $\pi^0\pi^0$ analysis which combined with a signal efficiency of 15.6% leads to the following final result:

$$\mathcal{B}(D^0 \to \pi^0\pi^0) = (0.084 \pm 0.001 \pm 0.004 \pm 0.003)\%$$

where the third error is due to the uncertainties in the normalization mode. In Fig. 1 (right) we show the invariant mass distribution of $D^0 \to \gamma\gamma$ candidates. There is no obvious signal and we find -6 ± 15 events which leads to an upper limit on the branching fraction of $< 2.2 \times 10^{-6}$ at the 90% confidence level. This is approximately an order of magnitude improvement over the PDG's current upper limit for $\mathcal{B}(D^0 \to \gamma\gamma)$ [6]. This analysis was published in PRD-RC [7], and formed the basis of J. Morris's (a graduate student supported by the Ohio State University) Ph.D. thesis.

References

[1] A. J. Bevin *et al.*, "The Physics of the B Factories," arXiv:1406.6311v2.

[2] `http://www.slac.stanford.edu/grp/rd/epac/Proposal/BaBarUpgrade_LST.pdf`

[3] A.J. Edwards *et al.*, "Radiation Monitoring with CVD Diamonds in BaBar," Nucl. Inst. Meth. **A552**, 176 (2005).

[4] G. Burdman, E. Golowich, J. L. Hewett, and S. Pakvasa, Phys. Rev. D **66**, 014009 (2002).

[5] S. Prelovsek and D. Wyler, Phys. Lett. B **500**, 304 (1991).

[6] T. Coan *et al.*, Phys. Rev. Lett. **90** 101801 (2003).

[7] J. P. Lees *et al.*, Phys. Rev. D **85**, 091107(R) (2012).

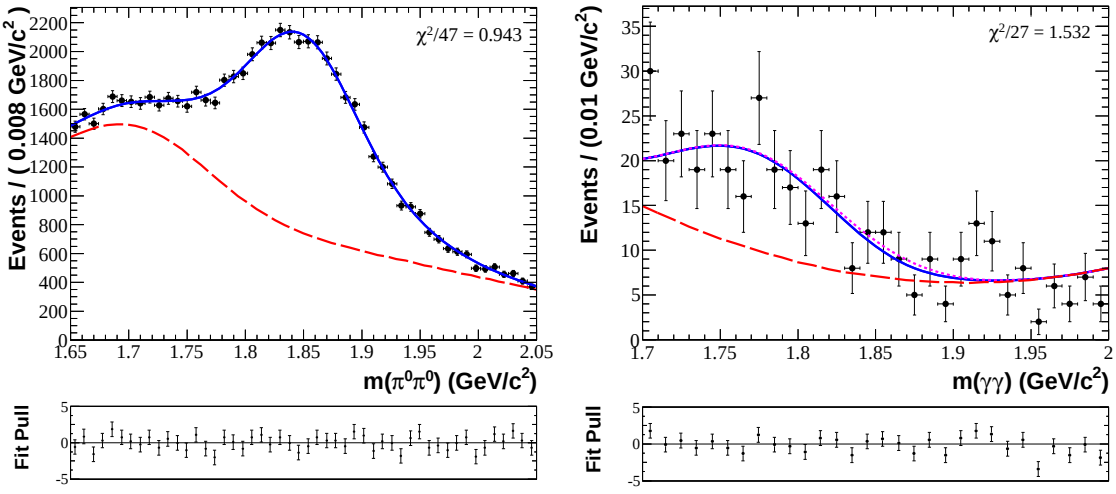

Figure 1: Invariant mass distribution for $D^0 \to \pi^0\pi^0$ candidates (left) and $D^0 \to \gamma\gamma$ candidates (right).

Final Report for the period 12/1/2010 – 4/30/2014

Contract DE-FG02-91ER40690

Cosmic Frontier: Dark Energy Experiments

Principle Investigator

Klaus Honscheid, Professor of Physics

Post-Doctoral Researchers

Dr. Eric Huff, Dr. Peter Melchior

Graduate Student Researchers

Ken Patton, Eric Suchyta

The Ohio State University
Department of Physics
191 West Woodruff Avenue
Columbus, Ohio 43210

July 2014

Overview

The Ohio State University Cosmic Frontier task has established a very strong presence in Dark Energy research. Led by K. Honscheid, the PI of this effort, the group contributed to the Baryon Oscillation Spectroscopic Survey (BOSS), the Dark Energy Survey (DES) and the Dark Energy Spectroscopic Instrument (DESI). Below we list our major accomplishments on these experiments over the lifetime of the grant.

- Design and construction of the BOSS data acquisition system.
- Development, construction and operation of the DECam readout and control system.
- Leadership of the DES science verification effort.
- Service work for the DES collaboration. The PI is the DES System Scientist, serves on the management and executive committees and chairs the DES publication board. Group members chair analysis subgroups and the early career committee.
- DES analysis projects in the area of weak gravitational lensing and the large-scale structure of the universe. Lead authors of the first DES science publication.
- Level-2 lead for the DESI instrument control system.
- Service work for the DESI collaboration including serving on the executive committee and the technical board.

Introduction

In 1998/99, two research groups independently discovered through the observation of Type Ia supernovae that the expansion of the Universe accelerates [1]. This acceleration suggests the existence of an energy density component which acts against gravity, the so-called dark energy. In the framework of the ΛCDM concordance model of cosmology, dark energy (Λ) represents approximately 68% of the total energy density; in addition, the Universe consists of 27% cold dark matter (CDM), baryonic matter (5%) and a negligible amount of radiation, mainly photons from the Cosmic Microwave Background (CMB). Whereas the latter two components are well understood, the dark universe remains a mystery. The physical nature of dark matter and especially dark energy is not described by the standard model of particle physics. Experimentally, the most promising opportunities to answer these fundamental questions are offered by large sky surveys. The roadmap for dark energy experiments has been defined by the 2006 Dark Energy Task Force (Albrecht et al. 2006) and was further refined by the 2010 Astronomy decadal survey [2] and the 2012 DOE Dark Energy Community Study [3]. The recommended series of experiments in a staged approach was strongly endorsed by the recent Community Summer Study (Snowmass) [4]. The OSU Cosmic Frontier program is well aligned with this approach. We are members of the Dark Energy Survey (DES) and the Baryon Oscillation Spectroscopic Survey (BOSS), the two mid-size, Stage III projects that are now operational. In addition, we are contributing to the development of the DESI project which will be one of the first Stage IV dark energy experiments.

Dark Energy Survey and Dark Energy Camera

DES is a large sky survey aimed directly at understanding the mysteries of the dark universe. The survey uses a powerful new instrument, the Dark Energy Camera (DECam), which was installed last year on the Blanco 4-meter telescope at the Cerro Tololo Inter-American Observatory (CTIO) in the Chilean mountains. Over five years, the DES collaboration will use 525

nights to image 5000 square degrees of the sky in five optical filter bands. The primary science goal is to understand the properties of dark energy using four complementary techniques: galaxy cluster counts, weak lensing, angular power spectrum and type Ia supernovae. The survey started August 31, 2013.

SISPI – The DECam Data Acquisition System

A major responsibility of the OSU Cosmic Frontier task is the DES mountain-top data acquisition system (Survey Image System Process Integration or SISPI). SISPI is implemented as a distributed multi-processor system with a software architecture based on the Client-Server and Publish-Subscribe design patterns. The underlying message passing protocol is based on PYRO, a powerful distributed object technology system written entirely in Python. A distributed shared variable system was added to support exchange of telemetry data and other information between different components of the system.

For the last 5 years the DES/DECam data acquisition system has been a major component of our research effort. Honscheid is the Level 2 project manager and OSU systems engineer Ann Elliott is the lead software developer on the project. Most of the SISPI work was done at OSU. Our group developed the infrastructure and communication software, the components of the image acquisition pipeline, parts of the instrument control system and all the interactive tools for the observer including the observer console and image displays. Graduate student K. Patton led the development of data quality assessment tools. Graduate student E. Suchyta wrote the instrument control code for the filter changer and the hexapod. He also developed the tools used by all observers to write exposure scripts. For SISPI we have combined traditional astronomical instrument control systems with ideas found in particle physics data acquisition systems. The success of this project has been widely recognized and we have been invited to present our work at many international conferences (SPIE 2014, 2012, 2010 and 2008; AAS; DPF; APS; IEEE-NSS 2009 and 2008; Realtime 2012 and 2007).

SISPI was completed in time for DECam commissioning in 2012. The system worked exceedingly well. By December we typically enjoyed uptimes of 98% and higher, which is quite an achievement for a system of this complexity. Not unlike particle physics experiments SISPI records a large number of operational and environmental parameters in a database. This information archive quickly became a critical resource to solve problems during commissioning and science verification. Building the observer console and other user interfaces on a web-based platform was another successful design choice.

DES Science Verification

A second major focus of our group's activities was DES science verification (SV). The SV period followed DECam commissioning and lasted from November 2012 until the end of the DES observing time in February 2013. At a reduced scale it continued through the community observing time until June 2013. The SV program was designed to establish that the instrument, telescope, and data handling systems were producing imaging data of sufficient quality to execute the Dark Energy Survey. An important additional goal was to test and to improve operational efficiency to ensure that the DES collaboration can make optimal use of its allocated time once the survey starts. All members of our task made significant contribution to this program. K. Honscheid led the project together with G. Bernstein (U. of Pennsylvania). They

developed the observing and analysis plans and organized a team of DES members with expertise in observing, astronomical instrumentation, image processing and the DES science program. Over a period of 23 nights and 57 half nights we collected data to assess the delivered image quality, the photometric calibration, and the long term stability of key parameters such as the readout noise, gain and linearity. For 32 of these nights, a member of the OSU group was part of the observing team on Cerro Tololo.

DES Science

Our interest in DECam is motivated by the exciting science program of the Dark Energy Survey. Parallel to our instrumentation activities and our contributions to science verification, we have developed a strong effort in dark energy science with a special focus on weak gravitational lensing and large scale structure. A primary objective is to constrain cosmological parameters, in particular those related to dark energy, from second-order shear statistics. These statistics quantify the correlation of an excess ellipticity (shear) of galaxies, which is introduced by the fact that light of distant galaxies is distorted (sheared) by the tidal gravitational field of foreground matter structures. The strength of this correlation can be related to the evolution of the matter density field of the Universe, which again can be related to a specific set of cosmological parameters and dark energy models.

Weak Lensing Analysis of DES Science Verification Data

Led by post-doctoral researcher P. Melchior, the entire group is conducting the first DES weak lensing analysis using observations of five massive galaxy cluster fields, taken during science verification in November - December 2012. We measured the mass and cluster galaxy distributions of five massive galaxy clusters observed during the Science Verification phase of the Dark Energy Survey, with the purpose of 1) validating DECam for task of measuring weak-lensing shapes, and 2) providing mass and cluster galaxy maps covering 1.5 sq. degrees (corresponding to linear scales of 10-24 Mpc at the cluster redshifts). For this purpose, we

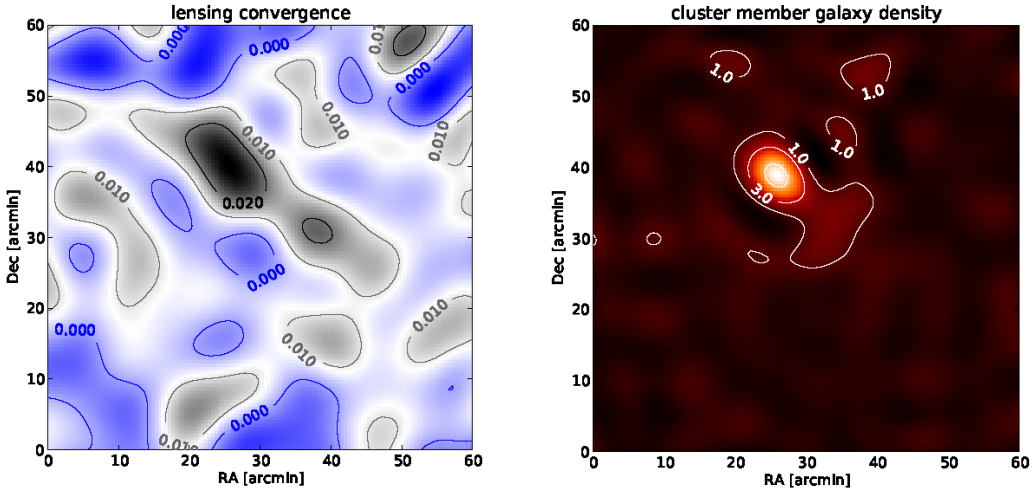

Figure 1 (Left) Preliminary maximum-likelihood mass reconstruction of the weak-lensing convergence of the galaxy cluster RXC J2248.7-4431. (Right) Cluster member distribution of the same cluster as detected by the red-sequence cluster finder RedmaPPer

established a data processing pipeline that is capable of producing science-grade co-added

images from DECam data. We conducted a series of rigorous tests on astrometry, photometry, image quality, PSF modeling, and shear measurement accuracy to single out flaws in the data but also to identify the optimal data processing steps and parameters. The results of this work have been submitted for publication in MNRAS.

Magnification

Weak gravitational lensing measurements are typically only based on the shear component of the gravitational lensing distortion. Lensing shear is generally accompanied by magnification, causing a change in the observed sizes and fluxes of background galaxies of similar strength to the shear. Traditional attempts to detect magnification have focused on the changes in the number of galaxies behind massive known lenses [5]. Due to the large variations in galaxy luminosities these measurements have been much noisier than shear results. E. Huff demonstrated that well-known scaling relations between certain galaxy properties can significantly improve this situation. One particularly well-studied relationship is that between the size, the surface brightness, and the concentration of the galaxy light profile [6]. Knowledge of the latter two, which are unaffected by lensing, allows one to predict the size of a galaxy; deviation from the predicted size is an estimator for magnification with measurement noise that is much smaller than the intrinsic scatter in galaxy sizes. Using this scaling relation, E. Huff performed a magnification measurement using SDSS data with roughly half the statistical power of a shear measurement [7]. There is evidence that much of the remaining noise in the magnification estimator can be removed with better quality imaging [8]. We are planning to repeat this measurement with DES, and preliminary work on size magnification has already been done by members of this group. The early results are promising. We have confirmed that a photometric fundamental plane similar to that seen in SDSS is present in the DES Science Verification data. If the observed scatter proves to be representative, then the signal-to-noise per galaxy from magnification in DES with this technique is comparable to that of the shear. In addition to improving the statistical power of weak lensing measurements, a combined shear and magnification analysis may pay significant dividends in terms of reducing the systematic error budget of DES. We are currently modifying our tools such as the simulation package described above and the DEIMOS [9] weak lensing pipeline developed by P. Melchior to exploit these scaling relations for a competitive DES magnification measurement. Huff will lead the early DES science program for this category of measurement. He is also the co-convener of the DES magnification working group.

BOSS and DESI

BOSS [10] is the flagship project of SDSS-III, the successor to the highly successful Sloan Digital Sky Survey (SDSS). BOSS carries out a spectroscopic survey of 1.6 million luminous red galaxies out to redshift $z = 0.75$ and 160,000 high redshift quasars. The primary goal of BOSS is a measurement of the expansion history of the Universe using baryon acoustic oscillations - a standard ruler imprinted in the clustering of galaxies and the intergalactic medium. The size of this signature in the early Universe is known with great precision from CMB measurements. The project is well underway and on target to meet all science goals by the scheduled project end date in 2014. Ohio State University is an institutional member of the SDSS-III collaboration. David Weinberg (OSU Astronomy) is the SDSS-III project scientist, and members of the OSU

Cosmic Frontier group joined the BOSS instrumentation team and contributed to the upgrade of the SDSS spectrographs. Our principle contributions were the production of the BOSS front end electronics and the design and construction of a new data acquisition system. Honscheid was named a BOSS Architect. Last year, BOSS published the most precise BAO result to date for a redshift z=0.57 and the first dark energy measure for z>2 corresponding to a time when the expansion of the Universe was still decelerating [11, 12].

The success of the BOSS survey has demonstrated the robustness of the BAO technique and it has been realized that this method can be extended to reach a precision on dark energy measurements and constraints previously thought possible only with space based missions. Following recommendations by the 2010 Decadal Survey and the 2012 Dark Energy community task force report [3], an even larger spectroscopic survey called DESI is under development [13]. DESI is a Stage IV ground based dark energy experiment to study baryon acoustic oscillations and the growth of structure with a 14,000 – 18,000 deg^2 survey using the Mayall telescope on Kitt Peak. The project received CD-0 approval from the DOE and is aiming for a CD-1 review in January 2014. Honscheid is one of eight members of the DESI steering committee. The group prepared a site analysis for the DOE and is now focusing on the conceptual design report. Honscheid and Huff were Co-PIs on a NOAO observing proposal that was awarded several nights with DECam and the Blanco to obtain galaxy and QSO targets for DESI. Building on the expertise in online systems for astronomical instruments gained with DES and BOSS our group will lead the development of the DESI readout and control system.

Bibliography and References Cited

[1] S. Perlmutter et al., ApJ 517 565 (1999) and A. G. Riess et al, AJ 116 1009 (1998)

[2] A. Albrecht et al, arXiv:astro-ph/0609591 (2006)

[3] A. Albrecht, S. Dodelson et al., “Community Dark Energy Task Force Report," http://science.energy.gov/hep/hepap/meetings/20120827 (2012)

[4] S. Dodelson, K. Honscheid, “Dark Energy and CMB”, Snowmass 2013 proceedings.

[5] R. Scranton et al., ApJ 633, 589 (2005)

[6] J. Ford et al, ApJ 754, 143 (2012), M. Watanabe, K. Kodaira, S. Okamura, ApJ 292, 73 (1985) and A. W. Graham, MNRAS 334, 859 (2002)

[7] E. M. Huff and G. J. Graves, submitted to ApJL, arXiv:111.1070 (2011)

[8] F. Schmidt et al. ApJ 744, L22 (2012)

[9] P. Melchior et al., MNRAS 412, 1552 (2011)

[10] K. Dawson et al, Astronomical Journal 145 10 (2013)

[11] L. Anderson et al., MNRAS 428, 1036 (2013)

[12] N. G. Busca et al, Astronomy & Astrophysics, Volume 552, id.A96 (2013)

[13] D. Schlegel et al., arXiv:0904.0468v3 (2009), F. Abdalla et. al., arXiv:1209.2451 (2012)